This is the Pre-Published Version.

This version of the article has been accepted for publication, after peer review (when applicable) and is subject to Springer Nature's AM terms of use (https://www.springernature.com/gp/open-research/policies/accepted-manuscript-terms), but is not the Version of Record and does not reflect post-acceptance improvements, or any corrections. The Version of Record is available online at: http://dx.doi.org/10.1007/s10915-024-02682-3.

Constrained Mix Sparse Optimization via Hard Thresholding Pursuit

Xinlin Hu[a,b], Yaohua Hu[c], Xiaoqi Yang[b], and Kai Zhang[d,e]

[a]School of Mathematics and Statistics, Guangdong University of Technology, Guangzhou 510520, P. R. China
[b]Department of Applied Mathematics, The Hong Kong Polytechnic University, Kowloon, Hong Kong
[c]School of Mathematical Sciences, Shenzhen University, Shenzhen 518060, P. R. China
[d]School of Finance, Guangdong University of Finance and Economics, Guangzhou 510320, P. R. China
[e]Shenzhen Audencia Financial Technology Institute, Shenzhen University, Shenzhen 518060, P. R. China

Abstract

Mix sparse structure, namely the sparse structure appearing in the inter-group and intra-group manners simultaneously, is inherited in a wide class of practical applications. Hard thresholding pursuit (HTP) is a practical and efficient algorithm for solving a least square problem with cardinality constraint. In this paper, we propose an algorithm based on HTP to solve a constrained mix sparse optimization problem, named MixHTP, and establish its linear convergence property under the restricted isometry property. Moreover, we apply the MixHTP to compressive sensing with simulated data and enhanced indexation with real data. Numerical results exhibit an excellent performance of MixHTP on approaching a solution with mix sparse structure and MixHTP outperforms several state-of-the-art algorithms in the literature.

Keywords: Hard thresholding pursuit Mix sparse structure Restricted isometry property Convergence property Enhanced indexation

1 Introduction

In the past few decades, sparse optimization has attracted a great amount of attention from researchers in a wide range of fields, such as compressive sensing [13], bioinformatics [34] and finance management [4]. In many applications, the underlying sparse solution $\bar{x}$ can be uncovered by an underdetermined linear system: $b = Ax + \varepsilon$, where the sensing matrix $A \in \mathbb{R}^{m\times n}(m \ll n)$ and the observation vector $b \in \mathbb{R}^m$ are known and the noise vector ε is unknown. The sparsity of a vector x means the number of nonzero components in x, which is denoted by the ℓ_0-norm $\|x\|_0$. In this paper we assume that x has a disjoint group structure: $x := (x_{\mathcal{G}_1}^\top, \cdots, x_{\mathcal{G}_N}^\top)^\top$, that is $\cup_{i=1}^N \mathcal{G}_i = [n]$ (where $[n] := \{1, \cdots, n\}$), and $\mathcal{G}_i \cap \mathcal{G}_j = \emptyset$ for any $i, j \in [N]$ and $i \neq j$. A nonzero group $\mathcal{G}_j$ is one where one of the entries in $x_{\mathcal{G}_j}$ is nonzero. The group sparsity of vector

x means the number of nonzero groups in x, denoted by the $\ell_{2,0}$-norm $\|x\|_{2,0} := \sum_{i=1}^N \|x_{\mathcal{G}_i}\|_2^0$ (with the convention $0^0 = 0$).

Depending on the practical sparsity requirements on the variable x, the following (group) sparse optimization problems have been investigated respectively in the literature:

$$\min_{x\in\mathbb{R}^n} \|Ax - b\|^2 \quad \text{s.t. } \|x\|_0 \le s, \tag{1}$$

$$\min_{x\in\mathbb{R}^n} \|Ax - b\|^2 \quad \text{s.t. } \|x\|_{2,0} \le S, \tag{2}$$

where s and S are the required sparsity and group sparsity of x respectively. See [8, 17, 19, 44, 45] for applications of the model (1) in compressive sensing and [7, 15, 23, 25, 33] for applications of the model (2) in multiple measurement vector problem and bioinformatics. Inspired by the ideas of greedy methods for sparse optimization, several low-complexity and greedy algorithms have been developed, such as orthogonal matching pursuit (OMP) [45], adaptive forward-backward greedy algorithm [44], iterative hard thresholding (IHT) [8] and hard thresholding pursuit (HTP) [17] for solving the problem (1), and blockOMP [15], groupIHT [25] and simultaneousHTP [7] for solving the problem (2) respectively. Under the assumption of restricted isometry property (RIP) and group RIP, their convergence guarantees are established in [17, 19, 45] and in [7, 33] respectively.

Lagrange sparse variants including lower order $\ell_q(0 < q < 1)$ regularization problems, relevant constrained ones of (1) and (2) and their group sparse variants have been considered in [22, 23, 39, 42, 43] by virtue of ℓ_q norm $\|x\|_q := \left(\sum_{i=1}^n |x_i|^q\right)^{1/q}$ $(0 < q)$ and $\ell_{p,q}$ norm $\|x\|_{p,q} := \left(\sum_{j=1}^N \|x_{\mathcal{G}_j}\|_p^q\right)^{1/q}$ $(0 \le q \le 1 \le p \le 2)$. On the other hand, inspired by Lasso and group Lasso, mix sparse optimization models were considered in terms of composition of $\|x\|_1$ and $\|x\|_{2,1}$, see [14, 37]. In particular, the following SGLasso is proposed in [37]:

$$\min_{x\in\mathbb{R}^n} \|Ax - b\|^2 + (1-\alpha)\lambda\|x\|_{2,1} + \alpha\lambda\|x\|_1, \tag{3}$$

where $\alpha \in [0, 1]$ is used to balance the $\ell_{2,1}$ and ℓ_1 norm penalties.

It is known that the ℓ_1 regularization problem shows disappointing numerical performance [23, 42, 44], and introduces extra bias in estimation [3, 29]. Numerous studies on lower-order regularization problems with $q = 1/2$ show their better numerical performance than the ℓ_1 regularization problem, e.g., in [23, 34, 42]. It has been revealed that among ℓ_q and $\ell_{p,q}$ regularized problems, $\ell_{1/2}$ and $\ell_{2,1/2}$ ones are most efficient in numerical performance.

The formulations (1) and (2) with either sparsity or inter-group sparsity alone may not delight some practical applications. Sometimes the intra-sparsity in the selected groups is also significant. In the gene expression data of bioinformatics [37], the groups may be gene pathways and both the sparsity of the groups (pathways) and the sparsity within each group are required, while the latter is to identify particularly important genes in the selected pathways of interest. In portfolio selection [14, 41], the groups may be the industrial sectors and can be used to characterize the diversity of the portfolio, while the constraint on the overall sparsity of the portfolio allows the investor to limit the total number of the selected assets. In these applications, the sparse solution enjoys a mix sparse structure, which adopts both the inter-group sparsity and the intra-group sparsity simultaneously.

Moreover, sparse optimization problems with a non-negative constraint or a convex constraint have also been investigated in recent literature [6, 28, 31, 38, 46]. An orthogonal greedy algorithm for non-negative sparse recovery and an iterative re-weighted least squares algorithm for non-negative sparse and group sparse recovery were proposed in [28, 31] accordingly. Additionally, a variant of alternating direction method of multipliers was proposed in [38] for a non-negative sparse recovery, in which ℓ_1/ℓ_2 norm was applied to approximate ℓ_0 norm. Moreover, two variants of iterative hard thresholding method were proposed in [6,46] for sparse recovery under a class of convex constraint, which both combines smoothing approximation and extrapolation technique.

Therefore, in the present paper, we consider the following constrained mix sparse optimization problem:

$$\min_{x\in\mathbb{R}^n} \|Ax-b\|^2 \quad \text{s.t. } x\in\mathcal{M}\cap\mathcal{C}, \tag{4}$$

where $\mathcal{M} := \{x\in\mathbb{R}^n : \|x\|_0 \le s, \|x\|_{2,0} \le S\}$ is a set of the mix sparse structures and $\mathcal{C}\subseteq\mathbb{R}^n$ is a closed and convex set. Inspired by the idea of HTP [17], this paper aims to propose an efficient first-order algorithm to solve problem (4) with a linear convergence property. There are two major difficulties in problem (4) stemming from the coupling of the mix sparse constraint $\mathcal{M}$ and the closed and convex constraint $\mathcal{C}$ and that of sparsity and group sparsity in $\mathcal{M}$. Due to the introduction of the constraint set $\mathcal{C}$, a perturbation on the gradient descent step and a full support condition are introduced to guarantee that the least squares subproblem is feasible. The latter condition is satisfied when $\mathcal{C}$ is the non-negative constraint as in [28,31] and when $\mathcal{C}$ is the special set considered in the numerical examples section. Our algorithm is even new when there is only either sparsity or group sparsity requirement.

We carry out extensive numerical experiments on simulated data and compare MixHTP with many existing algorithms in the literature. We find that the MixHTP outperforms several state-of-the-art solvers in mix sparse optimization without constraint or with different polyhedral constraint $\mathcal{C}$. It is revealed that the MixHTP has high applicability to solve mix sparse optimization with constraint $\mathcal{C}$. Motivated by successful applications of mix sparsities in portfolio selection [14,41], we consider an application of MixHTP to enhanced indexation, which aims to construct a structured sparse portfolio with a higher return than the index. In practice, stocks in a sector/industry (i.e., GICS classification) usually have a tendency for selection in the market [35]; hence investors often trade stocks in a few sectors/industries. Numerical results on S&P indexes dataset show that the portfolio built by MixHTP achieves a higher annualized excess return and Sharpe ratio.

We use $\sharp(\cdot)$ and $\sharp_G(\cdot)$ to denote the number of elements and groups in a set, respectively. Let $x\in\mathbb{R}^n$ have a group structure $x := (x_{\mathcal{G}_1}^\top, \cdots, x_{\mathcal{G}_N}^\top)^\top$ with group size $n_i := \sharp(\mathcal{G}_i)$, and denote the index sets of its nonzero entries of x and nonzero groups of $(x_{\mathcal{G}_1}^\top, \cdots, x_{\mathcal{G}_N}^\top)^\top$ by $\mathrm{supp}(x)$ and G-$\mathrm{supp}(x)$, respectively. The capital Greek letters $\Gamma, \Lambda, \Phi, \Psi$ are used to denote the index sets, and x_Γ and A_Γ are used to denote the subvector of x indexed by Γ and the submatrix of A with columns in Γ, respectively. Let $\mathcal{G}_\Lambda := \cup_{i\in\Lambda}\mathcal{G}_i$. We use x_Γ^P to denote the projection of x onto the subspace of $\mathbb{R}^n$ indexed by Γ, that is, the elements indexed by Γ are kept and the rest are set to zero. Moreover, we use $\Gamma\oplus\Lambda$ to denote the symmetric difference of the sets Γ and Λ, that is, $\Gamma\oplus\Lambda := (\Gamma\setminus\Lambda)\cup(\Lambda\setminus\Gamma)$. As usual, I represents an identity matrix, $\mathbf{0}$ and $\mathbf{1}$ denote the vectors of zeros and ones, respectively, and $\|x\|$ and $\|A\|_2$ denote the Euclidean norm of vector x and the spectral norm of matrix A, respectively.

The rest of the paper is organized as follows. We recall the notions of RIP and group RIP and discuss their properties in Section 2. A general framework of MixHTP for solving problem (4) is proposed in Section 3. The convergence properties on approximate and exact recovery of the MixHTP are analyzed in Section 4, as well as the high probability of successful recovery when A is a random Gaussian matrix. Numerical results of the MixHTP on simulated data and application to sparse enhanced indexation with real data are presented in Section 5. A conclusion is given in Section 6.

2 Restricted Isometry Property

2.1 RIP and GRIP

The restricted isometry property (RIP) [13] is widely used for the establishment of the oracle property and recovery bound for sparse optimization problems [10, 12], and the convergence analysis of sparse optimization algorithms [19, 30, 45].

Definition 2.1. *Let $s \in \mathbb{N}$. The matrix A is said to satisfy the s-restricted isometry property (for short, s-RIP) if there is some $\delta_s \in (0, 1)$ such that*

$$(1 - \delta_s)\|x_\Gamma\|^2 \leq \|A_\Gamma x_\Gamma\|^2 \leq (1 + \delta_s)\|x_\Gamma\|^2,$$

for any $x \in \mathbb{R}^n$ and $\Gamma \subseteq [n]$ with $\sharp(\Gamma) \leq s$. The s-restricted isometry constant (for short, s-RIC) is the smallest constant δ_s such that the s-RIP is satisfied.

Some useful properties of the RIP are listed in Lemma 2.1 below, of which the results were presented in [30, Proposition 3.2] and [19, Lemmas 6.16 and 6.20] for the case when $\mu = 1$. As the proofs for the general μ are similar to that when $\mu = 1$ and the details of the proofs are omitted.

Lemma 2.1. *Suppose that A satisfies s-RIP with $\delta_s \in (0, 1)$. Let $u, v \in \mathbb{R}^n$, $\varepsilon \in \mathbb{R}^m$, $\Gamma \subseteq [n]$, and $\mu \in (0, \frac{1}{1-\delta_s}]$. Then the following assertions are true.*

(i) *If $\sharp(\Gamma) \leq s$, then*
$$\|I - \mu A_\Gamma^\top A_\Gamma\|_2 \leq 1 - \mu + \mu\delta_s.$$

(ii) *If $\sharp(\mathrm{supp}(u) \cup \mathrm{supp}(v)) \leq s$, then*
$$|\langle u, (I - \mu A^\top A)v\rangle| \leq (1 - \mu + \mu\delta_s)\|u\|\|v\|.$$

(iii) *If $\sharp(\Gamma \cup \mathrm{supp}(v)) \leq s$, then*
$$\|((I - \mu A^\top A)v)_\Gamma\| \leq (1 - \mu + \mu\delta_s)\|v\|.$$

(iv) *If $\sharp(\Gamma) \leq s$, then*
$$\|(A^\top \varepsilon)_\Gamma\| \leq \sqrt{1 + \delta_s}\|\varepsilon\|.$$

A natural extension of RIP to the group-RIP is introduced in [16, 24]. Its definition is recalled as follows.

Definition 2.2. *Let $S \in \mathbb{N}$. The matrix A is said to satisfy the S-group restricted isometry property (for short, S-GRIP) if there is some $\Delta_S \in (0, 1)$ such that*

$$(1 - \Delta_S)\|x_{\mathcal{G}_\Lambda}\|^2 \leq \|A_{\mathcal{G}_\Lambda} x_{\mathcal{G}_\Lambda}\|^2 \leq (1 + \Delta_S)\|x_{\mathcal{G}_\Lambda}\|^2,$$

for any $x \in \mathbb{R}^n$ and $\Lambda \subseteq [N]$ with $\sharp(\Lambda) \leq S$. The S-group restricted isometry constant (for short, S-GRIC) is the smallest constant Δ_S such that the S-GRIP is satisfied.

Extending Lemma 2.1 to group structure, some useful properties of the GRIP are provided in the following lemma.

Lemma 2.2. *Suppose that A satisfies S-GRIP with $\Delta_S \in (0, 1)$. Let $u, v \in \mathbb{R}^n$, $\varepsilon \in \mathbb{R}^m$, $\Lambda \subseteq [N]$, and $\mu \in (0, \frac{1}{1-\Delta_S}]$. Then the following assertions are true.*

(i) *If* $\sharp(\Lambda) \leq S$*, then*

$$\|I - \mu A_{\mathcal{G}_\Lambda}^\top A_{\mathcal{G}_\Lambda}\|_2 \leq 1 - \mu + \mu\Delta_S.$$

(ii) *If* $\sharp(\text{G-supp}(u) \cup \text{G-supp}(v)) \leq S$*, then*

$$|\langle u, (I - \mu A^\top A)v\rangle| \leq (1 - \mu + \mu\Delta_S)\|u\|\|v\|.$$

(iii) *If* $\sharp(\Lambda \cup \text{G-supp}(v)) \leq S$*, then*

$$\|((I - \mu A^\top A)v)_{\mathcal{G}_\Lambda}\| \leq (1 - \mu + \mu\Delta_S)\|v\|.$$

(iv) *If* $\sharp(\Lambda) \leq S$*, then*

$$\|(A^\top \varepsilon)_{\mathcal{G}_\Lambda}\| \leq \sqrt{1 + \Delta_S}\|\varepsilon\|.$$

Proof. (i) By definition of spectral norm, one has

$$\|I - \mu A_{\mathcal{G}_\Lambda}^\top A_{\mathcal{G}_\Lambda}\|_2 = \max_{x_{\mathcal{G}_\Lambda} \neq \mathbf{0}} \frac{\langle (I - \mu A_{\mathcal{G}_\Lambda}^\top A_{\mathcal{G}_\Lambda})x_{\mathcal{G}_\Lambda}, x_{\mathcal{G}_\Lambda}\rangle}{\|x_{\mathcal{G}_\Lambda}\|^2}.$$

Note that

$$\begin{aligned}\langle (I - \mu A_{\mathcal{G}_\Lambda}^\top A_{\mathcal{G}_\Lambda})x_{\mathcal{G}_\Lambda}, x_{\mathcal{G}_\Lambda}\rangle &= \|x_{\mathcal{G}_\Lambda}\|^2 - \mu\|A_{\mathcal{G}_\Lambda}x_{\mathcal{G}_\Lambda}\|^2 \\ &\leq (1 - \mu(1 - \Delta_S))\|x_{\mathcal{G}_\Lambda}\|^2,\end{aligned}$$

where the inequality follows from Definition 2.2 and $\sharp(\Lambda) \leq S$. Consequently, the conclusion follows.

(ii) Let $\Lambda := \text{G-supp}(u) \cup \text{G-supp}(v)$. Then we have $u_{\mathcal{G}_{\Lambda^c}} = \mathbf{0}$ and $v_{\mathcal{G}_{\Lambda^c}} = \mathbf{0}$, and hence

$$\begin{aligned}|\langle u, (I - \mu A^\top A)v\rangle| &= |\langle u_{\mathcal{G}_\Lambda}, (I - \mu A_{\mathcal{G}_\Lambda}^\top A_{\mathcal{G}_\Lambda})v_{\mathcal{G}_\Lambda}\rangle| \\ &\leq \|u_{\mathcal{G}_\Lambda}\|\|I - \mu A_{\mathcal{G}_\Lambda}^\top A_{\mathcal{G}_\Lambda}\|_2\|v_{\mathcal{G}_\Lambda}\| \\ &\leq (1 - \mu + \mu\Delta_S)\|u\|\|v\|,\end{aligned}$$

where the last inequality follows from assertion (i).

(iii) Note that

$$\begin{aligned}\|((I - \mu A^\top A)v)_{\mathcal{G}_\Lambda}\|^2 &= \langle ((I - \mu A^\top A)v)_{\mathcal{G}_\Lambda}^P, (I - \mu A^\top A)v\rangle \\ &\leq (1 - \mu + \mu\Delta_S)\|((I - \mu A^\top A)v)_{\mathcal{G}_\Lambda}^P\|\|v\|,\end{aligned}$$

where the inequality directly follows from (ii) by replacing u with $((I - \mu A^\top A)v)_{\mathcal{G}_\Lambda}^P$. Note that the assumption in (ii) is implied by $\sharp(\Lambda \cup \text{G-supp}(v)) \leq S$. Hence the conclusion follows.

(iv) It is proved in [1, Lemma 1]. □ □

These properties of s-RIP and S-GRIP will be helpful in convergence analysis of our proposed algorithm.

2.2 Connection between RIC and GRIC

By definitions of the RIC and GRIC, it is easy to verify the monotone property (one can also refer to [9, eq. (8)] and [1, pp. 17]):

$$\delta_\alpha \leq \delta_\beta \quad \text{and} \quad \Delta_\alpha \leq \Delta_\beta \quad \text{for any } \alpha \leq \beta. \tag{5}$$

Moreover, it is desirable to recall some connections between RIC and GRIC in the following proposition, which is taken from [16, pp. 5306] and [18, Proposition 1].

Proposition 2.1. *Given an arbitrary group index set* Λ *with* $\sharp(\Lambda) = S$, *let* $M := \sum_{i\in\Lambda} n_i$, *and* c_0 *be the greatest common divisor of* M *and* s. *Then*

$$\Delta_S \leq \delta_M \leq \frac{M - c_0}{s}\delta_{2s} + \frac{c_0}{s}\delta_s \leq \frac{M}{s}\delta_{2s}. \tag{6}$$

Remark 2.1. *A special case is the equisized group structure, that is,* $n_i \equiv \frac{n}{N}, \forall i = 1, \cdots, S$. *In this case,* $M = \frac{nS}{N}$ *and* (6) *is reduced to* $\Delta_S \leq \delta_{\frac{nS}{N}} \leq \frac{nS}{Ns}\delta_{2s}$. *This indicates that* Δ_S *is bounded by* δ_{2s} *with a factor of the ratio of group sparsity to sparsity.*

2.3 RIC for Gaussian Matrices

The RIC plays an important role in convergence analysis and estimating the convergence rate of sparse algorithms; see, e.g., [17, 19, 30, 44, 45]. The estimation of RIC depends on the assumed distribution of sensing matrix A. Now we provide the estimation of the RIC with high probability when A obeys a Gaussian distribution. It is worth noting that Gaussian distribution is elementary and widely discussed in portfolio theory [26, 27]. The general case of sub-Gaussian distribution is also provided in Remark 4.4. To this end, we recall a useful lemma from [40, Example 2.11].

Lemma 2.3. *Let* $A \in \mathbb{R}^{m\times n}$ *be a Gaussian matrix with each* $A_{ij} \sim \mathcal{N}(0, 1)$, $u \in \mathbb{R}^n$ *and* $w \in (0, 1)$. *Then*

$$\mathbb{P}(|m^{-1}\|Au\|^2 - \|u\|^2| \geq w\|u\|^2) \leq 2\exp\left(-\frac{mw^2}{8}\right).$$

Proposition 2.2. *Let* $A \in \mathbb{R}^{m\times n}$ *be a Gaussian matrix with each* $A_{ij} \sim \mathcal{N}(0, \frac{1}{m})$. *Let* $0 < \delta, t < 1$. *Then* A *satisfies the RIP and its RIC* $\delta_s < \delta$ *with probability at least* $1 - t$ *provided*

$$m \geq \frac{16}{3}\delta^{-2}\left(s(9 + 2\ln\frac{n}{s}) + 2\ln\frac{2}{t}\right).$$

By virtue of Lemma 2.3, the proof of Proposition 2.2 adopts a line of analysis similar to that of [19, Theorem 9.11]. The details are omitted.

3 Mix Hard Thresholding Pursuit

Hard thresholding pursuit (HTP) [7, 17] is a popular and practical algorithm for sparse optimization, which successively performs a gradient descent operator, a hard thresholding operator to select those variables with largest magnitudes, and a least square operator (also named pursuit) to debias the coefficient estimation. Motivated by the success of HTP and practical applications of the mix sparse structure, we propose an efficient algorithm named MixHTP to approach a solution of the mix sparse optimization problem (4).

Compared to sparse optimization problem (1) and group sparse optimization problem (2), there are two major difficulties in problem (4) stemming from coupling structures in its constraints. The first one is the coupling $\mathcal{M} \cap \mathcal{C}$ of the mix sparse constraint $\mathcal{M}$ and the general constraint $\mathcal{C}$. To deal with this difficulty, $\mathcal{M}$ and $\mathcal{C}$ are decoupled as the constraint of the hard thresholding operator and that of the least squares operator, respectively. The second one is the coupling of sparsity and group sparsity in $\mathcal{M}$. This coupling makes it difficult to obtain an analytical solution of the hard thresholding operator, that is the projection onto the mix sparse constraint, due to the mix and combinatorial natures of $\mathcal{M}$. To conquer this obstacle, a hard thresholding operator [17] and a group thresholding operator [7] are successively performed or vice versa for the mix sparse constraint $\mathcal{M}$. Therefore, the MixHTP consists of a gradient descent step, a combination of a hard thresholding operator and a group hard thresholding operator and a least squares operator on the constraint $\mathcal{C}$. In order that the constrained least squares subproblem is feasible, a perturbation is added to the gradient descent step and a full support condition of $\mathcal{C}$ is introduced. The latter condition is automatically satisfied when $\mathcal{C}$ is the non-negative constraint as in [28, 31] and when $\mathcal{C}$ is the special sets considered in the numerical examples section. The MixHTP algorithm is formulated as follows.

Algorithm 1 Mix Hard Thresholding Pursuit (MixHTP)

1: Initialize $x^0 \in \mathcal{C}$. Select constant stepsize $\mu > 0$ and parameter $r \in \{0, 1\}$.
2: If $\mathbf{0} \notin \mathcal{C}$, let $\omega > 0$; otherwise, let $\omega = 0$.
3: **for** $k = 1, 2, \ldots$ **do**
4: $\quad g^k := x^{k-1} - \mu A^\top(Ax^{k-1} - b)$.
5: $\quad$ **if** $g^k = \mathbf{0}$ **then**
6: $\quad\quad y^k := g^k + \frac{\omega}{\sqrt{n}}\mathbf{1}$.
7: $\quad$ **end if**
8: $\quad z^k := \mathcal{T}_{1-r}(\mathcal{T}_r(y^k))$.
9: $\quad x^k := \arg\min_{x\in\mathcal{C}}\{\|Ax - b\|^2 : \mathrm{supp}(x) \subseteq \mathrm{supp}(z^k)\}$.
10: $\quad$ **if** Stopping Criterion is satisfied **then**
11: $\quad\quad$ break
12: $\quad$ **end if**
13: **end for**

In the MixHTP, $\mathcal{T}_r$ represents the thresholding operator as

$$\mathcal{T}_r(x) := \begin{cases} \mathcal{H}(x; s), & \text{if } r = 0, \\ \mathcal{H}_G(x; S), & \text{if } r = 1, \end{cases} \tag{7}$$

where $\mathcal{H}(x; s)$ is the hard thresholding operator that sets all but the largest s elements (in absolute value) of x to zero [17], and $\mathcal{H}_G(x; S)$ is the group hard thresholding operator that sets all but the largest S groups (in Euclidean norm) of x to zero [25]. The least squares operator has a closed-form formula when the set $\mathcal{C}$ is the whole space or a simplex, but does not in general when there are additional non-negative constraints as in the case of numerical experiments in Section 5.

The small quantity $\frac{\omega}{\sqrt{n}}$ in line 6 is to prevent the emptiness case of the feasible set of the least squares subproblem when $x^{k-1} - \mu A^\top(Ax^{k-1} - b) = \mathbf{0}$ and $\mathbf{0} \notin \mathcal{C}$. In such a case the perturbation can guarantee that the subproblem in line 9 is feasible, under an additional full support condition of $\mathcal{C}$, namely $2^{[\mathcal{C}]} = 2^{[n]}$, where $2^{[\mathcal{C}]} := \{\mathcal{I} \subset [n] : \text{there is an } x \in \mathcal{C}, \text{ such that } \mathcal{I} = \mathrm{supp}(x)\}$ and $2^{[n]} := \{\emptyset \neq \mathcal{I} : \mathcal{I} \subseteq [n]\}$. See Lemma 3.1 below.

Lemma 3.1. *If $\mathbf{0} \in \mathcal{C}$ or the full support condition of $\mathcal{C}$ holds, then the subproblem in line 9 of Algorithm 1 has a non-empty feasible set.*

Proof. If $\mathbf{0} \in \mathcal{C}$, then the conclusion holds automatically. If $2^{[\mathcal{C}]} = 2^{[n]}$, then $\mathrm{supp}(z^k) \neq \emptyset$, as $y^k \neq \mathbf{0}$. By the assumption, there is an $x \in \mathcal{C}$ such that $\mathrm{supp}(x) = \mathrm{supp}(z^k)$. Thus the feasible set of the subproblem is non-empty. □ □

We present three examples to illustrate the operation of mix sparse operator. Assume that a vector $y \in \mathbb{R}^9$ with $N = 3$ equisized groups has a disjoint group structure $y = (y_{\mathcal{G}_1}^\top, y_{\mathcal{G}_2}^\top, y_{\mathcal{G}_3}^\top)^\top$, where $\mathcal{G}_1 = \{1, 2, 3\}$, $\mathcal{G}_2 = \{4, 5, 6\}$ and $\mathcal{G}_3 = \{7, 8, 9\}$. Considering the mix sparse operator with

$s = 4$ and $S = 2$, the outcomes for different y are presented in Table 1. These examples indicates that i) the outcome of $z = \mathcal{T}_{1-r}(\mathcal{T}_r(y))$ always satisfies $\|z\|_0 \le s$ and $\|z\|_{2,0} \le S$ whenever $r = 0$ or $r = 1$; and ii) mix sparse operator can only achieve the approximate projection onto $\mathcal{M}$.

Table 1: Illustrative example for mix sparse operator with $s = 4$ and $S = 2$.

$y \in \mathbb{R}^9$	Operator	$r = 0$	$r = 1$
Example 1			
$(\underbrace{1,2,3}_{\mathcal{G}_1},\underbrace{4,5,6}_{\mathcal{G}_2},\underbrace{7,8,9}_{\mathcal{G}_3})$	$\mathcal{T}_r(y)$	$(0,0,0,0,0,6,7,8,9)$	$(0,0,0,4,5,6,7,8,9)$
	$\mathcal{T}_{1-r}(\mathcal{T}_r(y))$	$(0,0,0,0,0,6,7,8,9)$	
Example 2			
$(\underbrace{1,8,9}_{\mathcal{G}_1},\underbrace{2,5,7}_{\mathcal{G}_2},\underbrace{3,4,6}_{\mathcal{G}_3})$	$\mathcal{T}_r(y)$	$(0,8,9,0,0,7,0,0,6)$	$(1,8,9,2,5,7,0,0,0)$
	$\mathcal{T}_{1-r}(\mathcal{T}_r(y))$	$(0,8,9,0,0,7,0,0,0)$	$(0,8,9,0,5,7,0,0,0)$
Example 3			
$(\underbrace{1,2,7}_{\mathcal{G}_1},\underbrace{4,5,6}_{\mathcal{G}_2},\underbrace{8,9,10}_{\mathcal{G}_3})$	$\mathcal{T}_r(y)$	$(0,0,7,0,0,0,8,9,10)$	$(0,0,0,4,5,6,8,9,10)$
	$\mathcal{T}_{1-r}(\mathcal{T}_r(y))$	$(0,0,7,0,0,0,8,9,10)$	$(0,0,0,0,0,6,8,9,10)$

Our algorithm is new even when only one of sparse constraint and group sparse constraint appears in (4). When $\mathcal{C} := \mathbb{R}^n$, Algorithm 1 reduces to HTP [17] for sparse optimization problem (1) (with $S = N$) and simultaneousHTP [7] for group sparse optimization problem (2) (with $s = n$) as special cases. Moreover, Algorithm 1 performs the mix hard thresholding as first $\mathcal{H}(x; s)$ and then $\mathcal{H}_G(x; S)$ when $r = 0$, and in reverse order when $r = 1$. For different r, we will present a general convergence property of MixHTP in Section 4, and the numerical performance of MixHTP in Section 5.

4 Convergence Analysis

This section is devoted to establishing convergence property of the MixHTP to an approximate or exact ground true solution under the s-RIP and S-GRIP assumptions. For the sake of simplicity, we write $\Xi^k := \text{supp}(z^k)$, define the constraint of line 9 in Algorithm 1 by $\Omega^k := \{x \in \mathcal{C} : \text{supp}(x) \subseteq \text{supp}(z^k)\}$, and introduce a correction of $\bar{x}$ to Ω^k by

$$e^k := \arg\inf_{e \in Z^k(\bar{x})} \|e\|, \tag{8}$$

where $Z^k(\bar{x}) := \{e \in \mathbb{R}^n : (\bar{x} + e)^P_{\Xi^k} \in \Omega^k\}$. Particularly, one can check

$$e^k = \mathbf{0} \quad \text{when } \mathcal{C} = \mathbb{R}^n \text{ or } \mathbb{R}^n_+, \tag{9}$$

by the fact that $(\bar{x})^P_{\Xi^k} \in \Omega^k$. In this section, we always use the following notations.

(H1) Let $\bar{x} \in \mathcal{M} \cap \mathcal{C}$ be a ground true solution of

$$b = A\bar{x} + \varepsilon, \tag{10}$$

with its support sets defined by

$$\bar{\Psi}_r := \begin{cases} \text{supp}(\bar{x}), & \text{if } r = 0, \\ \mathcal{G}_{\text{G-supp}(\bar{x})}, & \text{if } r = 1. \end{cases} \tag{11}$$

(H2) Let $\{x^k\}$, $\{y^k\}$ and $\{z^k\}$ be generated by Algorithm 1 with stepsize $\mu \in \left(0, \frac{1}{1-\min(\delta_{3s}, \Delta_{3S})}\right)$ and constant $\omega \in \mathbb{R}_+$, and support sets of $\mathcal{T}_r(y^k)$ and z^k be defined by

$$\Phi_r^k := \begin{cases} \text{supp}(\mathcal{T}_r(y^k)), & \text{if } r = 0, \\ \mathcal{G}_{\text{G-supp}(\mathcal{T}_r(y^k))}, & \text{if } r = 1, \end{cases} \tag{12}$$

and

$$\Psi_{1-r}^k := \begin{cases} \text{supp}(z^k), & \text{if } 1-r = 0, \\ \mathcal{G}_{\text{G-supp}(z^k)}, & \text{if } 1-r = 1. \end{cases} \tag{13}$$

By Algorithm 1 and (H2), one can check that

$$\Xi^k = \Phi_r^k \cap \Psi_{1-r}^k \quad \text{for } r \in \{0, 1\}.$$

Before presenting the Theorem 4.1, we start from the following three lemmas.

Lemma 4.1 (First thresholding)**.** *Let* $r \in \{0, 1\}$ *and* $d^k := (I - \mu A^\top A)(x^{k-1} - \bar{x})$. *Then*

$$\frac{1}{\sqrt{2}}\|(x^k - \bar{x})_{\bar{\Psi}_r \setminus \Phi_r^k}\| \leq \|d^k_{\bar{\Psi}_r \oplus \Phi_r^k}\| + \mu\|(A^\top \varepsilon)_{\bar{\Psi}_r \oplus \Phi_r^k}\| + \omega. \tag{14}$$

Proof. Fix $r = 0$. We know $\mathcal{T}_0(y^k) := \mathcal{H}(y^k; s)$ and thus $\|y^k_{\bar{\Psi}_0}\| \leq \|y^k_{\Phi_0^k}\|$. Then it follows that

$$\|y^k_{\bar{\Psi}_0 \setminus \Phi_0^k}\| \leq \|y^k_{\Phi_0^k \setminus \bar{\Psi}_0}\| \tag{15}$$

after eliminating the contribution on $\bar{\Psi}_0 \cap \Phi_0^k$. With the fact that $\bar{x}_{\Phi_0^k \setminus \bar{\Psi}_0} = \mathbf{0}$, we obtain

$$\|y^k_{\Phi_0^k \setminus \bar{\Psi}_0}\| = \|(y^k - \bar{x})_{\Phi_0^k \setminus \bar{\Psi}_0}\|. \tag{16}$$

Similarly, with the fact that $x^k_{\bar{\Psi}_0 \setminus \Phi_0^k} = \mathbf{0}$, we obtain

$$\|y^k_{\bar{\Psi}_0 \setminus \Phi_0^k}\| = \|(y^k - \bar{x} + \bar{x} - x^k)_{\bar{\Psi}_0 \setminus \Phi_0^k}\| \geq \|(\bar{x} - x^k)_{\bar{\Psi}_0 \setminus \Phi_0^k}\| - \|(y^k - \bar{x})_{\bar{\Psi}_0 \setminus \Phi_0^k}\|.$$

This, together with (16) and (15), implies

$$\|(\bar{x} - x^k)_{\bar{\Psi}_0 \setminus \Phi_0^k}\| \leq \sqrt{2}\|(y^k - \bar{x})_{\bar{\Psi}_0 \oplus \Phi_0^k}\|, \tag{17}$$

where the inequality holds because $\|x_\Lambda\| + \|x_\Gamma\| \leq \sqrt{2}\|x_{\Lambda \oplus \Gamma}\|$ for any $x \in \mathbb{R}^n$ whenever $\Lambda \cap \Gamma = \emptyset$. By line 4 and 6 in Algorithm 1 and (10), we have

$$\begin{aligned} y^k - \bar{x} &\leq x^{k-1} - \bar{x} - \mu A^\top(Ax^{k-1} - A\bar{x} - \varepsilon) + \frac{\omega}{\sqrt{n}}\mathbf{1} \\ &= d^k + \mu A^\top \varepsilon + \frac{\omega}{\sqrt{n}}\mathbf{1} \end{aligned} \tag{18}$$

(by definition of d^k). Hence (17) is reduced to

$$\begin{aligned}\|(\bar{x}-x^k)_{\bar{\Psi}_0\backslash\Phi_0^k}\| &\le \sqrt{2}\|(d^k+\mu A^\top\varepsilon+\frac{\omega}{\sqrt{n}}\mathbf{1})_{\bar{\Psi}_0\oplus\Phi_0^k}\| \\ &\le \sqrt{2}\left(\|d^k_{\bar{\Psi}_0\oplus\Phi_0^k}\|+\mu\|(A^\top\varepsilon)_{\bar{\Psi}_0\oplus\Phi_0^k}\|+\omega\right).\end{aligned}$$

The proof is similar when $r=1$. Then we conclude that (14) holds for $r\in\{0,1\}$. □ □

Lemma 4.2 (Second thresholding)**.** *Let* $r\in\{0,1\}$ *and* $d^k:=(I-\mu A^\top A)(x^{k-1}-\bar{x})$*. Denote by* $\Lambda_r^k:=\Phi_r^k\cap(\Psi_{1-r}^k\backslash\bar{\Psi}_{1-r})$ *and* $\Gamma_r^k:=\Phi_r^k\cap(\bar{\Psi}_{1-r}\backslash\Psi_{1-r}^k)$*. Then*

$$\frac{1}{\sqrt{2}}\|(x^k-\bar{x})_{\Gamma_r^k}\|\le\|d^k_{\Gamma_r^k\oplus\Lambda_r^k}\|+\mu\|(A^\top\varepsilon)_{\Gamma_r^k\oplus\Lambda_r^k}\|+\omega. \tag{19}$$

Proof. The proof is similar to the one in Lemma 4.1. Fix $r=0$. We know $\mathcal{T}_1(\mathcal{T}_0(y^k)):=\mathcal{H}_G(\mathcal{T}_0(y^k);S)$ and thus $\|[\mathcal{T}_0(y^k)]_{\bar{\Psi}_1}\|\le\|[\mathcal{T}_0(y^k)]_{\Psi_1^k}\|$. Then it follows by $\Phi_0^k=\mathrm{supp}(\mathcal{T}_0(y^k))$ from (12) that

$$\|y^k_{\Phi_0^k\cap(\bar{\Psi}_1\backslash\Psi_1^k)}\|\le\|y^k_{\Phi_0^k\cap(\Psi_1^k\backslash\bar{\Psi}_1)}\| \tag{20}$$

after eliminating the contribution on $\bar{\Psi}_1\cap\Psi_1^k$. Denote by $\Lambda_0^k:=\Phi_0^k\cap(\Psi_1^k\backslash\bar{\Psi}_1)$ and $\Gamma_0^k:=\Phi_0^k\cap(\bar{\Psi}_1\backslash\Psi_1^k)$. With the fact that $\bar{x}_{\Lambda_0^k}=\mathbf{0}$ and $x^k_{\Gamma_0^k}=\mathbf{0}$, we obtain

$$\|y^k_{\Lambda_0^k}\|=\|(y^k-\bar{x})_{\Lambda_0^k}\|\quad\text{and}\quad\|y^k_{\Gamma_0^k}\|\ge\|(\bar{x}-x^k)_{\Gamma_0^k}\|-\|(y^k-\bar{x})_{\Gamma_0^k}\|.$$

Combining these two inequalities, (20) reduces to

$$\|(\bar{x}-x^k)_{\Gamma_0^k}\|\le\sqrt{2}\|(y^k-\bar{x})_{\Gamma_0^k\oplus\Lambda_0^k}\|,$$

where the inequality holds because $\|x_\Lambda\|+\|x_\Gamma\|\le\sqrt{2}\|x_{\Lambda\oplus\Gamma}\|$ for any $x\in\mathbb{R}^n$ whenever $\Lambda\cap\Gamma=\emptyset$. It follows by (18) that

$$\begin{aligned}\|(\bar{x}-x^k)_{\Gamma_0^k}\| &\le \sqrt{2}\|(d^k+\mu A^\top\varepsilon+\frac{\omega}{\sqrt{n}}\mathbf{1})_{\Gamma_0^k\oplus\Lambda_0^k}\| \\ &\le \sqrt{2}\left(\|d^k_{\Gamma_0^k\oplus\Lambda_0^k}\|+\mu\|(A^\top\varepsilon)_{\Gamma_0^k\oplus\Lambda_0^k}\|+\omega\right).\end{aligned}$$

The proof is similar when $r=1$. Then we conclude that (19) holds for $r\in\{0,1\}$. □ □

Lemma 4.3 (Pursuit)**.** *The following assertions are true.*

(i) $\langle Ax^k-b,Ax^k-Ax\rangle\le 0$ *for any* $x\in\Omega^k$*.*

(ii) *Suppose that* $\delta_{2s}<1$*. Then*

$$\|x^k-\bar{x}\|\le\frac{\|(x^k-\bar{x})_{(\Xi^k)^c}\|}{\sqrt{1-\delta_{2s}^2}}+\frac{\sqrt{1+\delta_s}\|\varepsilon\|+2\|e^k\|}{1-\delta_{2s}}. \tag{21}$$

Proof. (i) It is a direct conclusion from the optimality condition of line 9 in Algorithm 1; see [5, Proposition 4.7.2].

(ii) Recall e^k be defined by (8). Note that

$$\begin{aligned}\|x^k-\bar{x}\|^2 &= \|(x^k-\bar{x})_{\Xi^k}\|^2+\|(x^k-\bar{x})_{(\Xi^k)^c}\|^2 \\ &\le (\|(x^k-\bar{x}-e^k)_{\Xi^k}\|+\|e^k\|)^2+\|(x^k-\bar{x})_{(\Xi^k)^c}\|^2,\end{aligned} \tag{22}$$

where the first term on the right hand side can be rewritten as

$$\|(x^k - \bar{x} - e^k)_{\Xi^k}\|^2 = \langle x^k - \bar{x} - e^k, (x^k - \bar{x} - e^k)^P_{\Xi^k} \rangle. \tag{23}$$

By (8), we have $(\bar{x} + e^k)^P_{\Xi^k} \in \Omega^k$, and then by Lemma 4.3(i),

$$\langle Ax^k - b, Ax^k - A(\bar{x} + e^k)^P_{\Xi^k} \rangle \leq 0. \tag{24}$$

Note by line 9 in Algorithm 1 that $x^k = (x^k)^P_{\Xi^k}$, and thus $x^k - (\bar{x} + e^k)^P_{\Xi^k} = (x^k - \bar{x} - e^k)^P_{\Xi^k}$. Due to this and (10), (24) is reduced to

$$\langle Ax^k - A\bar{x} - \varepsilon, A(x^k - \bar{x} - e^k)^P_{\Xi^k} \rangle \leq 0. \tag{25}$$

By (23) minus (25), we obtain

$$\begin{aligned} \|(x^k - \bar{x} - e^k)_{\Xi^k}\|^2 \leq &\langle x^k - \bar{x}, (I - A^\top A)(x^k - \bar{x} - e^k)^P_{\Xi^k} \rangle \\ &+ \langle A^\top \varepsilon - e^k, (x^k - \bar{x} - e^k)^P_{\Xi^k} \rangle. \end{aligned} \tag{26}$$

Noting by $\text{supp}(x^k) \subseteq \Xi^k$ that $\sharp(\text{supp}(x^k - \bar{x}) \cup \Xi^k) \leq 2s$, Lemma 2.1(ii) is applicable (with $x^k - \bar{x}$, $(x^k - \bar{x} - e^k)^P_{\Xi^k}$, 1, $2s$ in place of u, v, μ, s) to showing that

$$\langle x^k - \bar{x}, (I - A^\top A)(x^k - \bar{x} - e^k)^P_{\Xi^k} \rangle \leq \delta_{2s} \|x^k - \bar{x}\| \|(x^k - \bar{x} - e^k)_{\Xi^k}\|. \tag{27}$$

On the other hand, one has

$$\begin{aligned} \langle A^\top \varepsilon - e^k, (x^k - \bar{x} - e^k)^P_{\Xi^k} \rangle &= \langle (A^\top \varepsilon - e^k)_{\Xi^k}, (x^k - \bar{x} - e^k)_{\Xi^k} \rangle \\ &\leq (\|(A^\top \varepsilon)_{\Xi^k}\| + \|e^k\|) \|(x^k - \bar{x} - e^k)_{\Xi^k}\|. \end{aligned} \tag{28}$$

Noting that $\sharp(\Xi^k) \leq s$, Lemma 2.1(iv) is applicable to showing that $\|(A^\top \varepsilon)_{\Xi^k}\| \leq \sqrt{1 + \delta_s} \|\varepsilon\|$. This, together with (26)-(28), implies

$$\|(x^k - \bar{x} - e^k)_{\Xi^k}\| \leq \delta_{2s} \|x^k - \bar{x}\| + \sqrt{1 + \delta_s} \|\varepsilon\| + \|e^k\|.$$

Consequently, by letting $\alpha := \sqrt{1 + \delta_s} \|\varepsilon\| + 2\|e^k\|$ and $\beta := \alpha^2 + \|(x^k - \bar{x})_{(\Xi^k)^c}\|^2$, (22) deduces that

$$(1 - \delta_{2s}^2) \|x^k - \bar{x}\|^2 - 2\alpha\delta_{2s} \|x^k - \bar{x}\| - \beta \leq 0.$$

Hence $\|x^k - \bar{x}\|$ is upper-bounded by the larger root of the equation $(1 - \delta_{2s}^2)t^2 - 2\alpha\delta_{2s} t - \beta = 0$, that is,

$$\begin{aligned} \|x^k - \bar{x}\| &\leq \frac{\alpha\delta_{2s} + \sqrt{\alpha^2\delta_{2s}^2 + \beta(1 - \delta_{2s}^2)}}{1 - \delta_{2s}^2} \\ &\leq \frac{\alpha(1 + \delta_{2s}) + \sqrt{1 - \delta_{2s}^2} \|(x^{k-1} - \bar{x})_{(\Xi^k)^c}\|}{1 - \delta_{2s}^2}, \end{aligned}$$

where the last inequality follows from the fact that

$$\sqrt{a^2 + b^2} \leq a + b \quad \text{for any } a, b \geq 0. \tag{29}$$

Then we conclude that (21) holds. □ □

The main theorem of this section is then as follows, in which a linear convergence to an approximate ground true solution is guaranteed under the s-RIP and S-GRIP assumptions for the noise-aware linear system.

Theorem 4.1 (Approximate recovery). *Let $\{x^k\}$ be generated by Algorithm 1 with stepsize $\mu \in \left(0, \frac{1}{1-\min(\delta_{3s},\Delta_{3S})}\right)$. Denote the maximum of $3s$-RIC and $3S$-GRIC of A by $\kappa := \max(\delta_{3s}, \Delta_{3S})$. Suppose that κ satisfies*

$$1 - \mu + \mu\kappa < \sqrt{\frac{1-\kappa^2}{8}}. \tag{30}$$

Moreover, writing $\rho := \frac{2\sqrt{2}(1-\mu)+\sqrt{2}\mu(\delta_{3s}+\Delta_{3S})}{\sqrt{1-\delta_{2s}^2}}$ and $C := \frac{\sqrt{2}\mu(\sqrt{1+\delta_{2s}}+\sqrt{1+\Delta_{2S}})}{\sqrt{1-\delta_{2s}^2}} + \frac{\sqrt{1+\delta_s}}{1-\delta_{2s}}$, we have $\rho \in (0,1)$, and $\{x^k\}$ approximates $\bar{x}$ with the following error bound:

$$\|x^k - \bar{x}\| \le \rho\|x^{k-1} - \bar{x}\| + C\|\varepsilon\| + \frac{2}{1-\delta_{2s}}\|e^k\| + \frac{2\sqrt{2}}{\sqrt{1-\delta_{2s}^2}}\omega. \tag{31}$$

Proof. Fix $r = 0$. Noting by (11) and line 9 in Algorithm 1 that

$$\begin{cases} \operatorname{supp}(\bar{x}) = \bar{\Psi}_0 \cap \bar{\Psi}_1, \\ \operatorname{supp}(x^k) \subseteq \Xi^k = \Phi_0^k \cap \Psi_1^k, \end{cases} \tag{32}$$

we obtain

$$\begin{aligned} \operatorname{supp}(x^k - \bar{x}) &\subseteq \operatorname{supp}(x^k) \cup \operatorname{supp}(\bar{x}) \subseteq (\Phi_0^k \cap \Psi_1^k) \cup (\bar{\Psi}_0 \cap \bar{\Psi}_1) \\ &\subseteq \Phi_0^k \cup \bar{\Psi}_0; \end{aligned}$$

thus

$$\|x^k - \bar{x}\|^2 = \|(x^k - \bar{x})_{\Phi_0^k \cup \bar{\Psi}_0}\|^2 = \|(x^k - \bar{x})_{\Phi_0^k}\|^2 + \|(x^k - \bar{x})_{\bar{\Psi}_0 \setminus \Phi_0^k}\|^2. \tag{33}$$

Moreover, it is clear from (32) that

$$\begin{aligned} \operatorname{supp}((x^k - \bar{x})_{\Phi_0^k}) &\subseteq \operatorname{supp}(x^k - \bar{x}) \subseteq (\Phi_0^k \cap \Psi_1^k) \cup (\bar{\Psi}_0 \cap \bar{\Psi}_1) \\ &\subseteq \bar{\Psi}_1 \cup \Psi_1^k; \end{aligned}$$

consequently, recall that $\Xi^k = \Phi_0^k \cap \Psi_1^k$, it holds that

$$\begin{aligned} \|(x^k - \bar{x})_{\Phi_0^k}\|^2 &= \|((x^k - \bar{x})_{\Phi_0^k})_{\bar{\Psi}_1 \cup \Psi_1^k}\|^2 \\ &= \|(x^k - \bar{x})_{\Xi^k}\|^2 + \|(x^k - \bar{x})_{\Phi_0^k \cap (\bar{\Psi}_1 \setminus \Psi_1^k)}\|^2. \end{aligned}$$

This, together with (33), yields that

$$\begin{aligned} \|(x^k - \bar{x})_{(\Xi^k)^c}\|^2 &= \|x^k - \bar{x}\|^2 - \|(x^k - \bar{x})_{\Xi^k}\|^2 \\ &= \|(x^k - \bar{x})_{\Phi_0^k \cap (\bar{\Psi}_1 \setminus \Psi_1^k)}\|^2 + \|(x^k - \bar{x})_{\bar{\Psi}_0 \setminus \Phi_0^k}\|^2; \end{aligned}$$

then it follows from (29) that

$$\|(x^k - \bar{x})_{(\Xi^k)^c}\| \le \|(x^k - \bar{x})_{\Phi_0^k \cap (\bar{\Psi}_1 \setminus \Psi_1^k)}\| + \|(x^k - \bar{x})_{\bar{\Psi}_0 \setminus \Phi_0^k}\|. \tag{34}$$

This, together with (14), (19) and $\Phi_0^k \cap (\bar{\Psi}_1 \oplus \Psi_1^k) \subseteq \bar{\Psi}_1 \oplus \Psi_1^k$, deduces that

$$\begin{aligned} \frac{1}{\sqrt{2}}\|(x^k - \bar{x})_{(\Xi^k)^c}\| \le\ & \|d^k_{\bar{\Psi}_1 \oplus \Psi_1^k}\| + \|d^k_{\bar{\Psi}_0 \oplus \Phi_0^k}\| \\ & + \mu\|(A^\top \varepsilon)_{\bar{\Psi}_1 \oplus \Psi_1^k}\| + \mu\|(A^\top \varepsilon)_{\bar{\Psi}_0 \oplus \Phi_0^k}\| + 2\omega. \end{aligned} \tag{35}$$

Finally, we estimate the right hand side of (35). One has by (11) that $\bar{\Psi}_0 = \mathrm{supp}(\bar{x})$, and by (32) that $\mathrm{supp}(x^{k-1}) \subseteq \Phi_0^{k-1}$. Hence we obtain

$$(\bar{\Psi}_0 \oplus \Phi_0^k) \cup \mathrm{supp}(x^{k-1} - \bar{x}) \subseteq \bar{\Psi}_0 \cup \Phi_0^k \cup \Phi_0^{k-1}.$$

Similarly, we have

$$(\bar{\Psi}_1 \oplus \Psi_1^k) \cup \mathcal{G}_{\text{G-supp}(x^{k-1}-\bar{x})} \subseteq \bar{\Psi}_1 \cup \Psi_1^k \cup \Psi_1^{k-1}.$$

These, together with definitions (11)-(13), imply that

$$\sharp((\bar{\Psi}_0 \oplus \Phi_0^k) \cup \mathrm{supp}(x^{k-1} - \bar{x})) \leq 3s,$$

and

$$\sharp_{\mathrm{G}}((\bar{\Psi}_1 \oplus \Psi_1^k) \cup \mathcal{G}_{\text{G-supp}(x^{k-1}-\bar{x})}) \leq 3S.$$

Combining these two inequalities, Lemma 2.1(iii) and Lemma 2.2(iii) are applicable to showing that

$$\|d^k_{\bar{\Psi}_1 \oplus \Psi_1^k}\| + \|d^k_{\bar{\Psi}_0 \oplus \Phi_0^k}\| \leq (2 - 2\mu + \mu(\delta_{3s} + \Delta_{3S}))\|x^{k-1} - \bar{x}\|.$$

Similarly by Lemma 2.1(iv) and Lemma 2.2(iv),

$$\|(A^\top \varepsilon)_{\bar{\Psi}_1 \oplus \Psi_1^k}\| + \|(A^\top \varepsilon)_{\bar{\Psi}_0 \oplus \Phi_0^k}\| \leq (\sqrt{1 + \delta_{2s}} + \sqrt{1 + \Delta_{2S}})\|\varepsilon\|.$$

Consequently, (35) is reduced to

$$\begin{aligned}\|(x^k - \bar{x})_{(\Xi^k)^c}\| \leq\ & \sqrt{2}(2 - 2\mu + \mu(\delta_{3s} + \Delta_{3S}))\|x^{k-1} - \bar{x}\| \\ & + \sqrt{2}\mu(\sqrt{1 + \delta_{2s}} + \sqrt{1 + \Delta_{2S}})\|\varepsilon\| + 2\sqrt{2}\omega,\end{aligned}$$

and we conclude by (21) that (31) holds. The proof is similar when $r = 1$. Moreover, by monotone property $\delta_{2s} \leq \delta_{3s}$ (see (5)) and by assumption (30), one can check that $\rho \in (0, 1)$. □ □

Remark 4.1. *From the proof of Theorem 4.1, denoting $\Lambda_r^k := \bar{\Psi}_r \oplus \Phi_r^k$ and $\Gamma_r^k := \bar{\Psi}_r \oplus \Psi_r^k$, it is worth noting that one also has*

$$\begin{aligned}\|x^k - \bar{x}\| \leq \sqrt{\frac{2}{1 - \delta_{2s}^2}} \Big(&\|d^k_{\Lambda_r^k}\| + \|d^k_{\Phi_r^k \cap \Gamma_{1-r}^k}\| \\ & + \mu\|(A^\top \varepsilon)_{\Lambda_r^k}\| + \mu\|(A^\top \varepsilon)_{\Phi_r^k \cap \Gamma_{1-r}^k}\| + 2\omega\Big) + E,\end{aligned} \tag{36}$$

where $E := \frac{\sqrt{1+\delta_s}\|\varepsilon\| + 2\|e^k\|}{1-\delta_{2s}}$. Specifically, when $r = 1$, by (11), (12) and (13) it follows that $\Phi_1^k \cap \Psi_0^k = \Psi_0^k$. Therefore

$$\sharp_G(\Lambda_1^k) \leq 2S, \text{ and } \sharp(\Phi_1^k \cap \Gamma_0^k) \leq 2s;$$

when $r = 0$, we know that Γ_1^k denotes the index sets of groups and that

$$\sharp(\Lambda_0^k) \leq 2s, \text{ and } \sharp(\Phi_0^k \cap \Gamma_1^k) \leq s.$$

For any group index set Λ with $\sharp(\Lambda) = 2S$, denote by $M_{2S} := \sum_{i \in \Lambda} n_i$. By Proposition 2.1, Lemma 2.1(iii)-(iv) and Lemma 2.2(iii)-(iv), (36) *is reduced to*

$$\|x^k - \bar{x}\| \leq \sqrt{\frac{2}{1 - \delta_{2s}^2}} \left(\rho_r \|x^{k-1} - \bar{x}\| + \mu C_r \|\varepsilon\| + 2\omega\right) + E,$$

where

$$\rho_1 := 2-2\mu+\mu(\delta_{M_{2S}}+\delta_{2s}),\ C_1 := \sqrt{1+\delta_{M_{2S}}}+\sqrt{1+\delta_{2s}},$$

and

$$\rho_0 := 2-2\mu+\mu(\delta_s+\delta_{2s}),\ C_0 := \sqrt{1+\delta_s}+\sqrt{1+\delta_{2s}},$$

respectively. Clearly $\rho_1 > \rho_0$ and $C_1 > C_0$ when $M_{2S} \geq s$. Thus MixHTP with $r = 0$ enjoys a smaller upper bound for $\|x^k - \bar{x}\|$. This is consistent with the numerical experiment for the simulated data that a better performance is obtained for $r = 0$ than that for $r = 1$ (see Section 5.1).

Remark 4.2 (Large samplesize)**.** *Let $\mathcal{C} := \mathbb{R}^n$ or $\mathbb{R}^n_+$. It is clear by* (9) *that $e^k = \mathbf{0}$ and by Algorithm 1 that $\omega = 0$. We consider objective function $\frac{1}{m}\|Ax-b\|^2$ in* (4) *and select constant stepsize $\mu \equiv 1$ in Algorithm 1. Let $A \in \mathbb{R}^{m\times n}$ be a Gaussian matrix with each $A_{ij} \sim \mathcal{N}(0,1)$, and ε be a Gaussian noise with each $\varepsilon_i \sim \mathcal{N}(0,\sigma^2)$. Denote by $\nu := \sqrt{\frac{n}{m}} + \frac{1}{16}$. One can obtain by [40, Example 6.2] that*

$$\left\|I - \frac{A^\top A}{m}\right\|_2 \leq 2\nu + \nu^2, \tag{37}$$

with probability at least $1 - 2\exp(-\frac{m}{512})$. Furthermore, given a constant $c_1 > 1$, it can be shown by [21, Example 11.1] that

$$\left\|\frac{A^\top \varepsilon}{m}\right\|_\infty \leq 2\sigma\sqrt{\frac{c_1 \log n}{m}}, \tag{38}$$

with probability at least $1 - 2n^{1-2c_1}$ for $n > 1$. For any group index set Λ with $\sharp(\Lambda) = 2S$, denote by $M_{2S} := \sum_{i\in\Lambda} n_i$. With a similar line to the proof of Theorem 4.1, since $\|x\|_2 \leq \sqrt{d}\|x\|_\infty$ for any $x \in \mathbb{R}^d$, one can achieve that

$$\|x^k - \bar{x}\| \leq \left\|I - \frac{A^\top A}{m}\right\|_2 \|x^k - \bar{x}\| + \sqrt{s}\left\|\frac{A^\top \varepsilon}{m}\right\|_\infty + \|(x^k - \bar{x})_{(\Xi^k)^c}\|, \tag{39}$$

and

$$\frac{1}{\sqrt{2}}\|(x^k - \bar{x})_{(\Xi^k)^c}\| \leq 2\left\|I - \frac{A^\top A}{m}\right\|_2 \|x^{k-1} - \bar{x}\| + (\sqrt{2s} + \sqrt{M_{2S}})\left\|\frac{A^\top \varepsilon}{m}\right\|_\infty.$$

Combining this with (39), (37) *and* (38) *are applicable to showing that*

$$\|x^k - \bar{x}\| \leq (\nu^2 + 2\nu)\|x^k - \bar{x}\| + 2\sqrt{2}(\nu^2 + 2\nu)\|x^{k-1} - \bar{x}\| + 2\sigma c_2\sqrt{\frac{c_1 \log n}{m}}, \tag{40}$$

where $c_2 := 3\sqrt{s} + \sqrt{2M_{2S}}$. We have $\nu^2 + 2\nu \to \frac{33}{256}$ and $\sqrt{\frac{c_1 \log n}{m}} \to 0$, as $m \to \infty$. Then (40) *is reduced to*

$$\|x^k - \bar{x}\| \leq \tilde{\rho}\|x^{k-1} - \bar{x}\|,$$

where $\tilde{\rho} := \frac{66\sqrt{2}}{223} \in (0,1)$.

Remark 4.3. *Theorem 4.1 covers existing convergence theorems of HTP-types algorithms in the literature. Particularly, as mentioned before, when $\mathcal{C} := \mathbb{R}^n$ and $S = N$, Algorithm 1 is reduced to HTP [17] for sparse optimization; in this case, $e^k = \mathbf{0}$ and $\omega = 0$, and Theorem 4.1 (with $\mu \equiv 1$) is reduced to [17, Theorem 3.8]:*

$$\|x^k - \bar{x}\| \leq \sqrt{\tfrac{2\delta_{3s}^2}{1-\delta_{2s}^2}}\|x^{k-1} - \bar{x}\| + \tfrac{\sqrt{2(1-\delta_{2s})}+\sqrt{1+\delta_s}}{1-\delta_{2s}}\|\varepsilon\|.$$

When $\mathcal{C} = \mathbb{R}^n$, $s = n$ and $n_i \equiv \frac{n}{N}$, Algorithm 1 is reduced to simultaneousHTP [7] for joint sparse optimization; in this case, $e^k = \mathbf{0}$ and $\omega = 0$, and Theorem 4.1 is reduced to [7, Theorem 3].

Corollary 4.1 (Exact recovery)**.** *Let $\mathcal{C} := \mathbb{R}^n$ or $\mathbb{R}^n_+$, $\bar{x} \in \mathcal{M} \cap \mathcal{C}$ be an exact solution of $b = A\bar{x}$, and $\{x^k\}$ be generated by Algorithm 1 with stepsize $\mu \equiv 1$. Suppose that the maximum of $3s$-RIC and $3S$-GRIC of A satisfies*

$$\max(\delta_{3s}, \Delta_{3S}) < \frac{1}{3}. \tag{41}$$

Then $\{x^k\}$ approximates $\bar{x}$ with the following error bound:

$$\|x^k - \bar{x}\| \le \rho \|x^{k-1} - \bar{x}\|,$$

where $\rho := \sqrt{\frac{2}{1-\delta_{2s}^2}}(\delta_{3s} + \Delta_{3S}) \in (0, 1)$.

Proof. Note by assumptions and (9) that $\varepsilon = \mathbf{0}$, $e^k = \mathbf{0}$ and $\omega = 0$. With constant stepsize $\mu \equiv 1$, the parameter ρ defined in Theorem 4.1 is reduced to $\sqrt{\frac{2}{1-\delta_{2s}^2}}(\delta_{3s} + \Delta_{3S})$, and $\rho \in (0, 1)$ holds by assumption (41). □ □

To make Theorem 4.1 more practical, we present the following corollaries, in which a simpler assumption based on $3s$-RIC, while $3S$-GRIC is not required, and the high probability of successful recovery for a Gaussian matrix are provided, respectively.

Corollary 4.2. *Let $\{x^k\}$ be generated by Algorithm 1 with $S \le N/3$ and stepsize $\mu \in \left(0, \frac{1}{1-\min(\delta_{3s}, \Delta_{3S})}\right)$. For any group index set Λ with $\sharp(\Lambda) = 3S$, write $\eta := \frac{1}{s}\sum_{i \in \Lambda} n_i$. Suppose that $3s$-RIC of A satisfies*

$$1 - \mu + \frac{\mu(1+\eta)}{2}\delta_{3s} < \sqrt{\frac{1-\delta_{3s}^2}{8}}, \tag{42}$$

Then $\{x^k\}$ approximates $\bar{x}$ with error bound (32).

Proof. By Proposition 2.1 and the monotone property (5), we have $\Delta_{3S} \le \eta\delta_{2s} \le \eta\delta_{3s}$; then the parameter ρ defined in Theorem 4.1 is reduced to

$$\rho \le \frac{2\sqrt{2}(1-\mu) + \sqrt{2}\mu(1+\eta)\delta_{3s}}{\sqrt{1-\delta_{3s}^2}}, \tag{43}$$

which is smaller than 1 by (42). □ □

Corollary 4.3. *Let $A \in \mathbb{R}^{m \times n}$ be a Gaussian matrix with each $A_{ij} \sim \mathcal{N}(0, \frac{1}{m})$, and $\{x^k\}$ be generated by Algorithm 1 with stepsize $\mu \equiv 1$ and $S \le N/3$. For any group index set Λ with $\sharp(\Lambda) = 3S$, write $\eta := \frac{1}{s}\sum_{i \in \Lambda} n_i$. Then $\{x^k\}$ approximates $\bar{x}$ with error bound (32), with probability at least $1 - t$ provided that*

$$m \ge 16(2(1+\eta)^2 + 1)\left(s(9 + 2\ln\frac{n}{3s}) + \frac{2}{3}\ln\frac{2}{t}\right). \tag{44}$$

Proof. Proposition 2.2 is applicable (with $\frac{1}{\sqrt{2(1+\eta)^2+1}}$, $3s$ in place of δ, s) to concluding that

$$\delta_{3s} < \frac{1}{\sqrt{2(1+\eta)^2+1}},$$

that is (42) with $\mu \equiv 1$, with probability at least $1 - t$. Consequently, the conclusion directly follows Corollary 4.2. □ □

Remark 4.4. *More generally, if A is a random matrix with each row being independent mean-zero sub-Gaussian with parameter σ and variance one (see [40, Definition 2.2]), then conclusion* (32) *also holds with probability at least $1-t$ provided that (by virtue of [19, Theorem 9.11] and [40, Example 2.12])*

$$m \geq 16\sigma^2(2(1+\eta)^2+1)\left(s(9+2\ln\frac{n}{3s})+\frac{2}{3}\ln\frac{2}{t}\right).$$

For the noise-free case when $\varepsilon = \mathbf{0}$ and $\mathcal{C} := \mathbb{R}^n$ or $\mathbb{R}^n_+$, we provide in the following corollary a faster linear convergence rate than that in Theorem 4.1; i.e., $\bar{\rho} \leq \rho$ by (45) and (5). This linear convergence theory will be further validated in numerical results in Section 5 that the convergence is achieved within only a few number of iterations.

Corollary 4.4 (Faster linear convergence rate)**.** *Let $\mathcal{C} := \mathbb{R}^n$ or $\mathbb{R}^n_+$, $\bar{x} \in \mathcal{M} \cap \mathcal{C}$ be an exact solution of $b = A\bar{x}$, and $\{x^k\}$ be generated by Algorithm 1 with stepsize $\mu \in \left(0, \frac{1}{1-\min(\delta_s,\Delta_S)}\right)$. Suppose that* (30) *is satisfied, and write*

$$\bar{\rho} := \frac{2\sqrt{2}(1-\mu)+\sqrt{2}\mu(\delta_s+\Delta_S)}{\sqrt{1-\delta_s^2}}. \tag{45}$$

Then $\bar{\rho} \in (0,1)$, and there exists $K \in \mathbb{N}$ such that

$$\|x^k - \bar{x}\| \leq \bar{\rho}\|x^{k-1} - \bar{x}\| \quad \textit{for each } k > K.$$

Proof. Note by assumptions and (9) that $\varepsilon = \mathbf{0}$, $e^k = \mathbf{0}$ and $\omega = 0$, and then Theorem 4.1 is applicable to concluding that $\rho < 1$ and

$$\|x^k - \bar{x}\| \leq \rho\|x^{k-1} - \bar{x}\| \quad \text{for each } k \in \mathbb{N}.$$

This says that $\{x^k\}$ converges to $\bar{x}$, and thus there exists $K \in \mathbb{N}$ such that $\text{supp}(\bar{x}) \subseteq \text{supp}(x^k)$ and $\text{G-supp}(\bar{x}) \subseteq \text{G-supp}(x^k)$ for each $k \geq K$. Otherwise, suppose that there exists $i \in \text{supp}(\bar{x}) \setminus \text{supp}(x^k)$ or $j \in \text{G-supp}(\bar{x}) \setminus \text{G-supp}(x^k)$, and let $\epsilon := \min_{i\in\text{supp}(\bar{x})} |\bar{x}_i|$. Then $\|x^k - \bar{x}\| \geq |\bar{x}_i| \geq \epsilon$ or $\|x^k - \bar{x}\| \geq \|\bar{x}_{\mathcal{G}_j}\| \geq \epsilon$, contradicting to the fact that $\{x^k\}$ converges to $\bar{x}$.

Therefore, in view of Algorithm 1, $\{x^k - \bar{x}\}_{k\geq K}$ must be (s, S)-mix sparse, that is $x^k - \bar{x} \in \mathcal{M}, \forall k \geq K$. Then, following a similar line to the proof of Theorem 4.1, and by the fact that $\varepsilon = \mathbf{0}$, $e^k = \mathbf{0}$ and $\omega = 0$, we achieve that $\|x^k - \bar{x}\| \leq \bar{\rho}\|x^{k-1} - \bar{x}\|$ for each $k > K$, where $\bar{\rho}$ is defined by (45). Moreover, it is easy to verify that $\bar{\rho} > 0$, and we have by the monotone property (5) that $\bar{\rho} \leq \rho < 1$. □ □

5 Numerical Experiments

This section aims to illustrate the numerical performance of MixHTP for mix sparse optimization problem (4), by comparing with several state-of-the-art algorithms on simulated data and applying to enhanced indexation in portfolio selection with real data. All numerical experiments are implemented in R (4.0.0) and performed on a personal desktop (Intel Core i5-8500, 3.00GHz, 8.00GB of RAM).

5.1 Numerical Simulation

Simulated data are generated as follows. We first randomly generate an i.i.d. Gaussian ensemble $A \in \mathbb{R}^{m\times n}$ satisfying $AA^\top = I$. For a mix sparse solution $\bar{x} = (\bar{x}_{\mathcal{G}_1}^\top, \cdots, \bar{x}_{\mathcal{G}_N}^\top)^\top \in \mathbb{R}^n$ with N disjoint equisized groups (unless otherwise stated), we randomly select S groups of them as active ones within each every component being an i.i.d. Gaussian ensemble. The observation b is generated by

$$b = A\bar{x} + \sigma\varepsilon,$$

where ε is a vector with each component drawn from the standard Gaussian distribution and σ is the noise level to be specified. In the numerical experiments, the problem size is set as $n = 1024$ and $m = 256$, the number of groups $N = 64$, and the noise level $\sigma = 0.001$. Denote the group size by $\bar{n} := \frac{n}{N} = 16$, and define γ the percentage of nonzero elements within each group, i.e.,

$$\gamma := \frac{s}{\bar{n}S} = \frac{3}{\eta}, \tag{46}$$

where $\eta := \frac{3}{s}\bar{n}S$ is the parameter defined in Corollary 4.3. In the implementation of MixHTP, we select an initial point $x_0 = \mathbf{0}$, the stopping criterion as $\|x^k - x^{k-1}\| \le 10^{-8}$, parameter $r = 0$ (unless otherwise indicated) and $\omega = 10^{-3}$ when $\mathbf{0} \notin \mathcal{C}$. Two main criteria to measure the performance of the solvers are the relative error RE $= \frac{\|x-\bar{x}\|}{\|\bar{x}\|}$ and the successful recovery rate, where the recovery is regarded as "success" if RE ≤ 0.02, and "failure" otherwise. The sparsity level means $\frac{s}{n}$.

In numerical simulations, we consider problem (4) for the cases when $\mathcal{C} := \mathbb{R}^n$, $\mathbb{R}^n_+$, $\mathcal{B}_1$, $\mathcal{B}_2$, $\mathcal{S}$ and $\mathcal{S} \cap \mathbb{R}^n_+$, respectively, where $\mathcal{B}_1 := \{x \in \mathbb{R}^n : \|x - \frac{a}{n^{2/3}}\mathbf{1}\|_{3/2} \le a\}$, $\mathcal{B}_2 := \{x \in \mathbb{R}^n : \|x - \frac{a}{n^{1/3}}\mathbf{1}\|_3 \le \sqrt{2}a\}$ and $\mathcal{S} := \{x \in \mathbb{R}^n : \mathbf{1}^\top x = a\}$. The major computational cost of Algorithm 1 relies on the pursuit on $\mathcal{C}$ at line 9. Fortunately, line 9 is a low dimensional optimization problem on an affine space $\{x \in \mathbb{R}^n : \text{supp}(x) \subseteq \Xi^k\}$ where $\Xi^k := \text{supp}(z^k)$ with the form as:

$$x^k_{\Xi^k} := \arg\min_{x\in\mathcal{C}} \|A_{\Xi^k}x - b\|^2. \tag{47}$$

We solve the subproblems (47) mainly by R *CVXR* [20] package. Specifically, subproblem (47) owns closed-form formula when $\mathcal{C} := \mathbb{R}^n$:

$$x^k_{\Xi^k} = (A_{\Xi^k}^\top A_{\Xi^k})^{-1}A_{\Xi^k}^\top b.$$

Moreover, when $\mathcal{C} := \mathcal{S}$, subproblem (47) can be solved via Karush-Kuhn-Tucker (KKT) condition:

$$\begin{bmatrix} 2A_{\Xi^k}^\top A_{\Xi^k} & \mathbf{1} \\ \mathbf{1}^\top & 0 \end{bmatrix} \begin{bmatrix} x^k_{\Xi^k} \\ \lambda \end{bmatrix} = \begin{bmatrix} 2A_{\Xi^k}^\top b \\ a \end{bmatrix}, \tag{48}$$

where λ is the Lagrange multiplier.

The running time of line 9 in Algorithm 1 for different constraints $\mathcal{C}$ is illustrated in Fig. 1. It is indicated that line 9 can be achieved easily within a quite short time except for the constraints $\mathcal{B}_1$ and $\mathcal{B}_2$. However, with the higher sparsity level and the more complicate constraint, the running time tends to increase.

5.1.1 Unconstrained case $\mathcal{C} := \mathbb{R}^n$

We carry out three experiments. The first experiment shows the convergence behavior of the MixHTP with different stepsize μ when sparsity level is 10%. The average of RE of 200 random trials along the number of iterations is shown in Fig. 2(a). It shows that the MixHTP converges

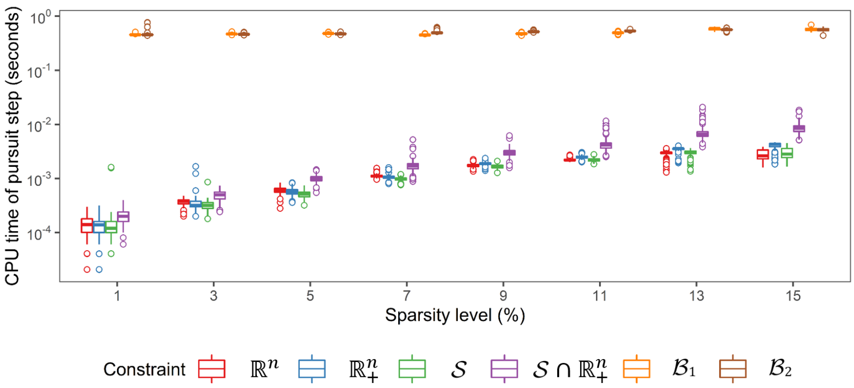

Figure 1: Running time of pursuit for different constraint $\mathcal{C}$.

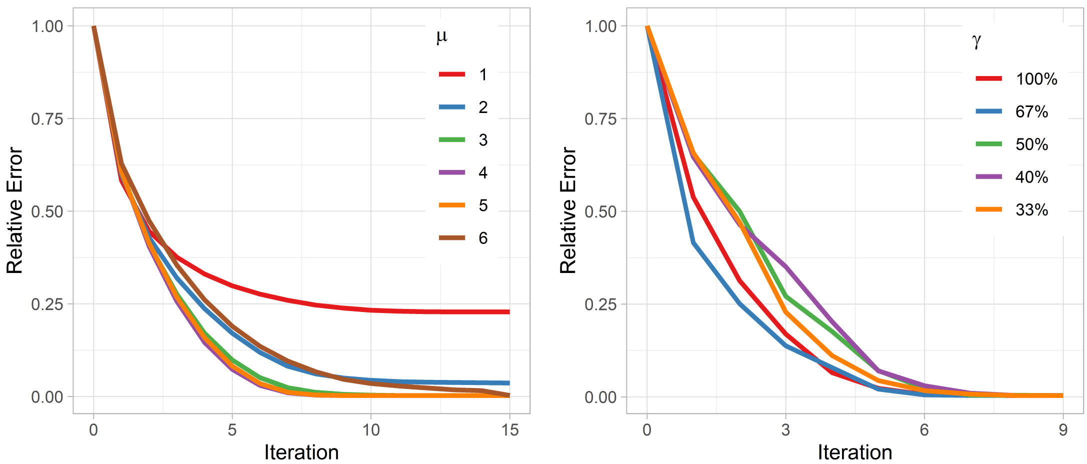

(a) Different μ

(b) Different γ

Figure 2: Convergence behavior of MixHTP.

to the true solution and the stepsize $\mu = 5$ has the best convergence performance; hence, we use the stepsize $\mu = 5$ in the following experiments. Fig. 2(b) also indicates that MixHTP converges within only a few number of iterations for different γ's.

The second experiment is to illustrate the sensitivity analysis of the MixHTP on intra-group and inter-group sparsity by varying the ratio γ from 100% to 33% and for equisized and non-equisized inter-group sparsity (The active groups are divided into two parts: half contain $s/4$ active entries, and the other half contain $3s/4$ active entries). As shown in Fig. 3, the MixHTP can achieve a high successful recovery rate for mix sparse optimization. It is also exhibited that the successful recovery rate is higher when γ is larger. This is consistent with Corollary 4.3 because the larger the γ, the smaller the η in (46), and thus less sample is required to achieve successful recovery; see (44).

The last experiment is implemented to compare the MixHTP with several state-of-the-art solvers in structured sparse optimization. Noted that solution $\bar{x}$ becomes a group sparse vector

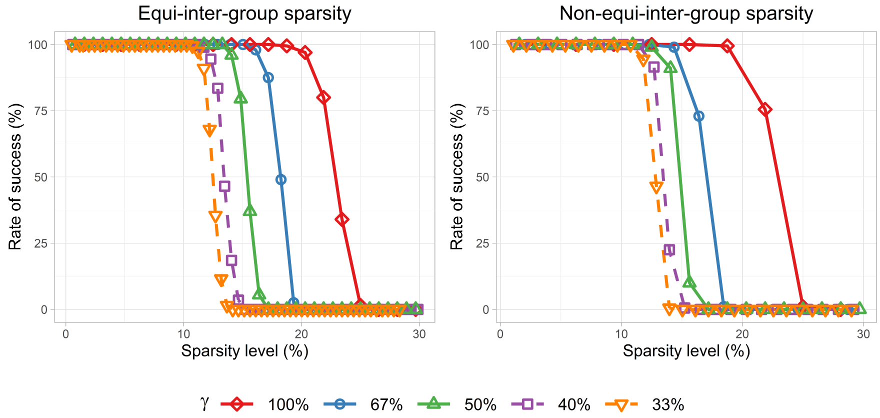

Figure 3: Sensitivity analysis of MixHTP for different γ.

Table 2: List of state-of-the-art algorithms for sparse learning.

Algorithm	Problem to be solved	Reference
Mix Hard Thresholding Pursuit (MixHTP)	Problem (4)	This paper
Mix Iterative Hard Thresholding (MixIHT)	Problem (4)	This paper
Group Hard Thresholding Pursuit (GroupHTP)	Problem (2)	[7]
Group Iterative Hard Thresholding (GroupIHT)	Problem (2)	[25]
Block Orthogonal Matching Pursuit algorithm (BlockOMP)	Problem (2)	[15]
Group Lasso (GLasso)	Problem (3) when $\alpha = 0$	[43]
Proximal Gradient Method with Group Half thresholding (PGM-GHalf)	Lagrange variants with $\ell_{2,1/2}$-norm	[23]
Sparse Group Lasso (SGLasso)	Problem (3)	[37]

when $\gamma = 100\%$. The solvers can be divided into two types due to the concerned structures: (i) group sparse solvers: GroupHTP [7], GroupIHT [25], BlockOMP [15], PGM-GSoft and PGM-GHalf [23]; and (ii) mix sparse solvers: MixHTP, MixIHT[1] (with $r = 0$ and $r = 1$) and SGLasso [37]; see Table 2 for details. When solving the mix sparse optimization problem with different γ, Fig. 4 shows that MixHTP (with $r = 0$) outperforms among these algorithms.

[1]MixIHT is an application of MixHTP by removing the pursuit step (i.e., line 9 in Algorithm 1), whose idea is inspired from [8, 25] and convergence theorem can be proved by following a line of analysis similar to Theorem 4.1.

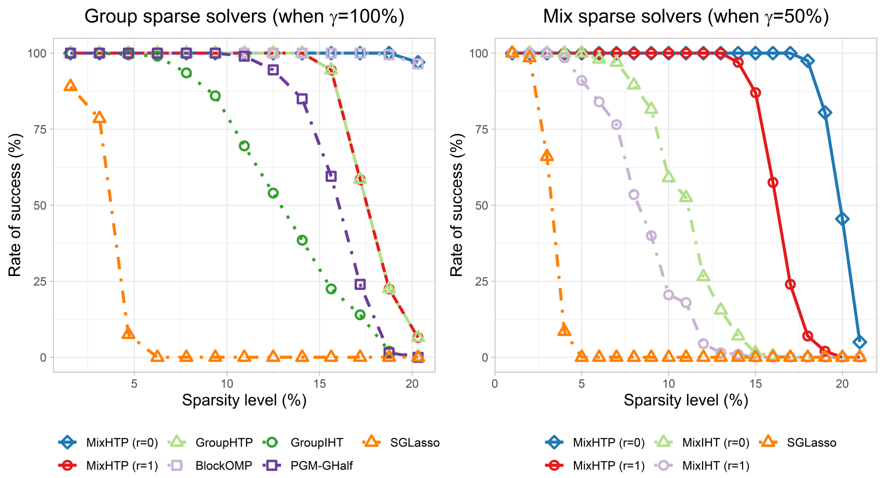

Figure 4: Sensitivity analysis of state-of-the-art sparse algorithms for different γ.

5.1.2 Convex constraint $\mathcal{C}$

Fig. 5 shows the sensitivity analysis of MixHTP for problem (4) under different constraint including $\mathcal{C} := \mathbb{R}^n_+$, $\mathcal{B}_1$, $\mathcal{B}_2$, $\mathcal{S}$ and $\mathcal{S} \cap \mathbb{R}^n_+$ (when $a = 10$). It is revealed that the MixHTP with different $\mathcal{C}$ owns a higher successful recovery rate with larger γ, and constraint $\mathcal{C} := \mathbb{R}^n_+$ shows a higher applicability to problem (4) than other constraints. Moreover, for the non-negative constraint $\mathcal{C} := \mathbb{R}^n_+$, we compare MixHTP with GroupHTPC[2], NNIRLS [28] and NNBOMP [32]. Fig. 6 indicates that the MixHTP has a high successful recovery rate and outperforms existing non-negative group sparse solvers.

5.2 Application to sparse enhanced indexation

In financial market, investors can make the profit from the price difference of the i-th stock with prices P^i_{t-1} at time $t-1$ and P^i_t at time t ($i = 1, \cdots, n$). We consider the i-th stock's rate of return r^i_t at time t to measure the profits with the form:

$$r^i_t := \frac{P^i_t - P^i_{t-1}}{P^i_{t-1}}.$$

The main purpose for investors is to find a portfolio (a combination of stocks) that would be possible to earn the profit in future based on history data. It is believed that the best portfolio is the one who can earn the same profit as the market index (i.e., S&P500 index), for instance, by replicating the performance of the index. The simple way to track the index is the portfolio constructed by all constituents of index with the same proportion. However, the high transaction cost and difficult practicability in real-life trading prompt investors to select a small number of constituents to mimic the performance of index, which is known as sparse index tracking [4]. Denote the simple rate of return of index and n constituents in the past T days by

$$\mathbf{r}^{\mathrm{I}} := [r^{\mathrm{I}}_1, r^{\mathrm{I}}_2, \cdots, r^{\mathrm{I}}_T]^\top \in \mathbb{R}^T,$$

[2]GroupHTPC is implemented for group sparse optimization (2) under constraint $\mathcal{C}$ by removing the thresholding operator $\mathcal{H}(x; s)$ in MixHTP.

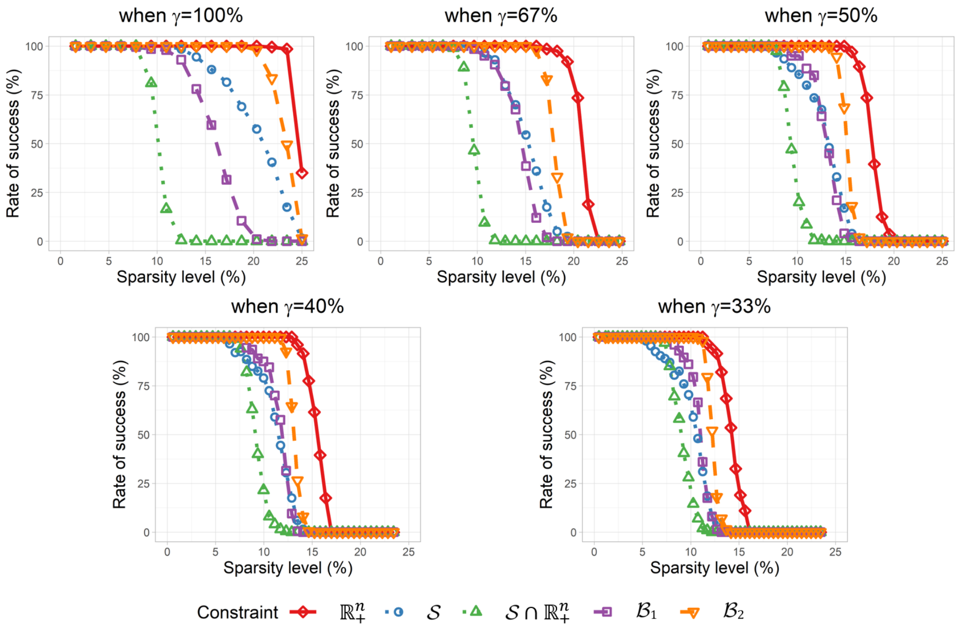

Figure 5: Sensitivity analysis of MixHTP for different constraint.

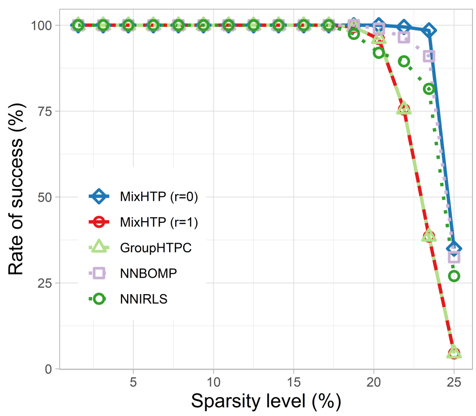

Figure 6: Sensitivity analysis of state-of-the-art group sparse algorithms for non-negative constraint when $\gamma = 100\%$.

and

$$\mathbf{R} := [\mathbf{r}^1; \mathbf{r}^2; \cdots; \mathbf{r}^n] \in \mathbb{R}^{T \times n},$$

respectively, where $\mathbf{r}^i := [r_1^i, r_2^i, \cdots, r_T^i]^\top \in \mathbb{R}^T$ denotes the return of i-th constituent. Hence, the sparse index tracking can be formulated under empirical tracking error through:

$$\min_{\mathbf{w}} \ f(\mathbf{w}) := \|\mathbf{r}^{\mathrm{I}} - \mathbf{R}\mathbf{w}\|^2, \text{ s.t. } \mathbf{w} \geq \mathbf{0}, \mathbf{1}^\top \mathbf{w} = 1, \|\mathbf{w}\|_0 \leq s,$$

Table 3: Performance evaluation criteria.

Criteria	Formula
Cumulative Return (CR_t)	$\sum_{i=1}^{t}(1+\mathcal{R}_i)-1$
Annualized Excess Return (AER)	$(\frac{\mathrm{CR}_T+1}{\mathrm{CR}_T^b+1})^{\frac{252}{T}}-1$
Annualized Standard Deviation (ASD)	$\sqrt{\frac{252}{T}\sum_{t=1}^{T}(\mathcal{R}_t-\mathbb{E}(\mathcal{R}))^2}$
Annualized Excess Sharpe Ratio (AESR)	AER / ASD
Worst Drawdown (WD)	$-\min(\frac{\mathrm{CR}_T}{\max_{t\in[0,T]}\mathrm{CR}_t}-1)$
Alpha and Beta in CAPM	$\mathcal{R}$ = Alpha + Beta $\times\mathcal{R}^b$

where $\mathbf{w}\in\mathbb{R}^n$ is the weight of constituents in outcome portfolio, and s represents the maximal number of selected constituents. This optimization problem and its variants are widely applied to track the index and solved by different algorithms; see [2, 4, 36] and the references therein.

Beyond index tracking, enhanced indexation aims to construct a portfolio that not only tracks but outperforms the index [11]. The excess return is typically defined as the portion of the portfolio return that exceeds the return of the index, and formulated mathematically as [47]

$$ER := \frac{1}{T}\mathbf{1}^\top(\mathbf{R}\mathbf{w}-\mathbf{r}^{\mathrm{I}}),$$

and hence the enhanced indexation is the trade-off between tracking error and excess return [2, 47]. Following a similar idea that the excess return is controlled by a desired value from [11], with budget and no-shorting constraints to mimic real-life trading, we consider the following formulation for sparse enhanced indexation:

$$\min_{\mathbf{w}}\ f(\mathbf{w}),\ \text{s.t. } \mathbf{w}\geq\mathbf{0}, \mathbf{1}^\top\mathbf{w}=1, \|\mathbf{w}\|_0\leq s, ER\geq\alpha^*,$$

where α^* denotes the minimal excess return of outcome portfolio.

The sector/industry information is now widely considered in portfolio management [14,35,41]. Inspired by the application to portfolio management with sector/industry information [14], we use ℓ_0 and $\ell_{2,0}$-norm to control the number of selected stocks and industries in outcome portfolio, respectively. Finally, we formulate the constrained mix sparse enhanced indexation as follows:

$$\min_{\mathbf{w}\in\mathcal{M}\cap\mathcal{C}}\ f(\mathbf{w}),$$

where $\mathcal{C} := \{\mathbf{w}\in\mathbb{R}^n_+ : \mathbf{1}^\top\mathbf{w}=1, ER\geq\alpha^*\}$.

In numerical experiment, we consider S&P500 index with its constituents that unchanged from 2015/01/02 to 2019/12/30. The daily price of the S&P500 dataset are downloaded from Yahoo Finance. Based on the Global Industry Classification Standard (GICS) to measure the group information, we collect the industry structure of constituents from Wikipedia[3], specifically, 61 industries are involved for 380 constituents.

[3]https://en.wikipedia.org/wiki/List_of_S%26P_500_companies

Table 4: Out-of-sample results.

	MixHTP ($r = 0$)	MixHTP ($r = 1$)	GroupHTPC	HTPC
α^*		0.01%		
AER	**0.0229**	0.0083	-0.0060	0.0112
ASD	0.1310	0.1311	**0.1302**	0.1307
AESR	**0.1747**	0.0633	-0.0458	0.0855
WD	**0.1675**	0.1767	0.1898	0.1750
Alpha(%)	**0.0114**	0.0055	-0.0001	0.0067
Beta	0.9445	0.9480	0.9444	0.9463
α^*		0.03%		
AER	0.0272	**0.0286**	0.0140	0.0176
ASD	0.1328	0.1320	0.1320	**0.1317**
AESR	0.2045	**0.2163**	0.1061	0.1339
WD	**0.1754**	0.1768	0.1904	0.1791
Alpha(%)	0.0125	**0.0131**	0.0073	0.0089
Beta	0.9581	0.9558	0.9585	0.9540
α^*		0.05%		
AER	0.0266	**0.0342**	0.0327	0.0171
ASD	0.1341	**0.1340**	0.1348	0.1342
AESR	0.1984	**0.2555**	0.2427	0.1274
WD	0.1897	**0.1874**	0.1958	0.1921
Alpha(%)	0.0122	**0.0151**	0.0139	0.0083
Beta	0.9612	0.9619	0.9747	0.9662
α^*		0.07%		
AER	0.0229	**0.0525**	0.0462	0.0248
ASD	0.1469	0.1413	0.1424	**0.1405**
AESR	0.1558	**0.3718**	0.3242	0.1763
WD	0.2320	**0.2022**	0.2093	0.2068
Alpha(%)	0.0107	**0.0207**	0.0175	0.0102
Beta	0.9770	0.9964	1.0154	0.9953
α^*		0.1%		
AER	0.0653	0.0715	**0.0735**	0.0571
ASD	0.1680	0.1606	**0.1550**	0.1654
AESR	0.3886	0.4453	**0.4742**	0.3454
WD	**0.2211**	0.2414	0.2352	0.2485
Alpha(%)	0.0210	0.0240	**0.0256**	0.0189
Beta	1.1228	1.0990	1.0737	1.1003

The whole period contains 1256 daily return rates of the index and its constituents. We regard the first 628 groups of return rates as in-sample dataset and the remained 628 groups as out-of-sample dataset. Given a fixed desired excess return α^*, the portfolio is constructed in in-sample dataset by training on first 70% dataset and testing on later 30% dataset with different combinations of two tuning parameters: sparsity s (from 10 to 200) and group sparsity S (from 5 to 30). We select the optimal tuning parameters that minimized the tracking error $f(\mathbf{w})$.

Given the portfolio return $\mathcal{R} := \{\mathcal{R}_1, \mathcal{R}_2, \ldots, \mathcal{R}_T\}$, the expected return $\mathbb{E}(\mathcal{R})$ can be estimated by the average of $\mathcal{R}$. We denote the return of S&P500 and its cumulative return by $\mathcal{R}^b$ and CR^b. Next we consider the criteria listed in Table 3 to compare the performance of different portfolios.

We compare the portfolio constructed by MixHTP with the one from GroupHTPC and HTPC[4]. We list the out-of-sample results for a series of $\alpha^* = 0.01\%, 0.03\%, 0.05\%, 0.07\%, 0.1\%$ in Table 4. The results demonstrate that MixHTP outperforms both GroupHTPC and HTPC in the majority of scenarios, while GroupHTPC exhibits superior performance when $\alpha^* = 0.1\%$. Additionally, it is worth noting that the AER, AESR and Alpha of portfolios in out-of-sample dataset tend to increase when considering a larger desired excess return α^*.

6 Conclusions

In this paper, by virtue of the mix structure and inspired by the idea of HTP, we proposed an algorithm MixHTP for solving a constrained mix sparse optimization problem. This problem includes constraints on inter-group sparsity, intra-group sparsity and a polyhedral constraint. Under the RIP-type assumption, we established the linear convergence property of the MixHTP to an approximate ground true solution. The MixHTP was then applied to compressive sensing with simulated data and enhanced indexation with real data. Numerical results demonstrated the outperformance of MixHTP and the superiority of mix sparse structure.

7 Acknowledgements

This work is supported by National Natural Science Foundation of China (12222112, 12071306, 32170655), Project of Educational Commission of Guangdong Province (2023ZDZX1017), Shenzhen Science and Technology Program (RCJC20221008092753082), Research Team Cultivation Program of Shenzhen University (2023QNT011), Guangdong Basic and Applied Basic Research Foundation (2023A1515012395) and Research Grants Council of Hong Kong (PolyU 15217520).

Declarations

Data Availability Statement

The authors will provide the test data if it is requested.

Conflict of interest

The authors declare that they have no conflict of interest.

[4]HTPC is implemented for sparse optimization (1) under constraint $\mathcal{C}$ by removing the thresholding operator $\mathcal{H}_G(x; S)$ in MixHTP.

References

[1] Baraniuk, R.G., Cevher, V., Duarte, M.F., Hegde, C.: Model-based compressive sensing. IEEE Transactions on Information Theory **56**(4), 1982–2001 (2010)

[2] Beasley, J.E., Meade, N., Chang, T.J.: An evolutionary heuristic for the index tracking problem. European Journal of Operational Research **148**(3), 621–643 (2003)

[3] Belloni, A., Chernozhukov, V.: Least squares after model selection in high-dimensional sparse models. Bernoulli **19**(2), 521–547 (2013)

[4] Benidis, K., Feng, Y., Palomar, D.P.: Sparse portfolios for high-dimensional financial index tracking. IEEE Transactions on Signal Processing **66**(1), 155–170 (2017)

[5] Bertsekas, D., Nedic, A., Ozdaglar, A.: Convex Analysis and Optimization. Athena Scientific (2003)

[6] Bian, W., Wu, F.: Accelerated smoothing hard thresholding algorithms for ℓ_0 regularized nonsmooth convex regression problem. Journal of Scientific Computing **96**(2), 33 (2023)

[7] Blanchard, J.D., Cermak, M., Hanle, D., Jing, Y.: Greedy algorithms for joint sparse recovery. IEEE Transactions on Signal Processing **62**(7), 1694–1704 (2014)

[8] Blumensath, T., Davies, M.E.: Iterative hard thresholding for compressed sensing. Applied and Computational Harmonic Analysis **27**(3), 265–274 (2009)

[9] Cai, T.T., Wang, L., Xu, G.: New bounds for restricted isometry constants. IEEE Transactions on Information Theory **56**(9), 4388–4394 (2010)

[10] Cai, T.T., Xu, G., Zhang, J.: On recovery of sparse signals via ℓ_1 minimization. IEEE Transactions on Information Theory **55**(7), 3388–3397 (2009)

[11] Canakgoz, N.A., Beasley, J.E.: Mixed-integer programming approaches for index tracking and enhanced indexation. European Journal of Operational Research **196**(1), 384–399 (2009)

[12] Candes, E.J., Romberg, J.K., Tao, T.: Stable signal recovery from incomplete and inaccurate measurements. Communications on Pure and Applied Mathematics: A Journal Issued by the Courant Institute of Mathematical Sciences **59**(8), 1207–1223 (2006)

[13] Candes, E.J., Tao, T.: Decoding by linear programming. IEEE Transactions on Information Theory **51**(12), 4203–4215 (2005)

[14] Chen, J., Dai, G., Zhang, N.: An application of sparse-group lasso regularization to equity portfolio optimization and sector selection. Annals of Operations Research **284**(1), 243–262 (2020)

[15] Eldar, Y.C., Kuppinger, P., Bolcskei, H.: Block-sparse signals: Uncertainty relations and efficient recovery. IEEE Transactions on Signal Processing **58**(6), 3042–3054 (2010)

[16] Eldar, Y.C., Mishali, M.: Robust recovery of signals from a structured union of subspaces. IEEE Transactions on Information Theory **55**(11), 5302–5316 (2009)

[17] Foucart, S.: Hard thresholding pursuit: An algorithm for compressive sensing. SIAM Journal on Numerical Analysis **49**(6), 2543–2563 (2011)

[18] Foucart, S.: Sparse recovery algorithms: Sufficient conditions in terms of restricted isometry constants. In: Approximation Theory XIII: San Antonio 2010, pp. 65–77. Springer (2012)

[19] Foucart, S., Rauhut, H.: A Mathematical Introduction to Compressive Sensing. Applied and Numerical Harmonic Analysis. Springer New York (2013)

[20] Fu, A., Narasimhan, B., Boyd, S.: CVXR: An R package for disciplined convex optimization. Journal of Statistical Software **94**, 1–34 (2020)

[21] Hastie, T., Tibshirani, R., Wainwright, M.: Statistical Learning with Sparsity: The Lasso and Generalizations. CRC Press (2015)

[22] Hu, Y., Hu, X., Yang, X.: On convergence of iterative thresholding algorithms to approximate sparse solution for composite nonconvex optimization. Mathematical Programming pp. 1–26 (2024)

[23] Hu, Y., Li, C., Meng, K., Qin, J., Yang, X.: Group sparse optimization via $\ell_{p,q}$ regularization. The Journal of Machine Learning Research **18**(1), 960–1011 (2017)

[24] Huang, J., Zhang, T.: The benefit of group sparsity. The Annals of Statistics **38**(4), 1978–2004 (2010)

[25] Jain, P., Rao, N., Dhillon, I.S.: Structured sparse regression via greedy hard thresholding. Advances in Neural Information Processing Systems **29** (2016)

[26] Kan, R., Smith, D.R.: The distribution of the sample minimum-variance frontier. Management Science **54**(7), 1364–1380 (2008)

[27] Kan, R., Zhou, G.: Optimal portfolio choice with parameter uncertainty. Journal of Financial and Quantitative Analysis **42**(3), 621–656 (2007)

[28] Majumdar, A.: Iterative re-weighted least squares algorithms for non-negative sparse and group-sparse recovery. In: ICASSP 2022-2022 IEEE International Conference on Acoustics, Speech and Signal Processing (ICASSP), pp. 4423–4427. IEEE (2022)

[29] Meinshausen, N., Yu, B.: Lasso-type recovery of sparse representations for high-dimensional data. The Annals of Statistics **37**(1), 246–270 (2009)

[30] Needell, D., Tropp, J.A.: Cosamp: Iterative signal recovery from incomplete and inaccurate samples. Applied and Computational Harmonic Analysis **26**(3), 301–321 (2009)

[31] Nguyen, T.T., Idier, J., Soussen, C., Djermoune, E.H.: Non-negative orthogonal greedy algorithms. IEEE Transactions on Signal Processing **67**(21), 5643–5658 (2019)

[32] O'Hanlon, K., Nagano, H., Keriven, N., Plumbley, M.D.: Non-negative group sparsity with subspace note modelling for polyphonic transcription. IEEE/ACM Transactions on Audio, Speech, and Language Processing **24**(3), 530–542 (2016)

[33] Qi, R., Yang, D., Zhang, Y., Li, H.: On recovery of block sparse signals via block generalized orthogonal matching pursuit. Signal Processing **153**, 34–46 (2018)

[34] Qin, J., Hu, Y., Xu, F., Yalamanchili, H.K., Wang, J.: Inferring gene regulatory networks by integrating ChIP-seq/chip and transcriptome data via lasso-type regularization methods. Methods **67**(3), 294–303 (2014)

[35] Sharma, A., Mehra, A.: Financial analysis based sectoral portfolio optimization under second order stochastic dominance. Annals of Operations Research **256**(1), 171–197 (2017)

[36] Shu, L., Shi, F., Tian, G.: High-dimensional index tracking based on the adaptive elastic net. Quantitative Finance **20**(9), 1513–1530 (2020)

[37] Simon, N., Friedman, J., Hastie, T., Tibshirani, R.: A sparse-group lasso. Journal of Computational and Graphical Statistics **22**(2), 231–245 (2013)

[38] Tao, M., Zhang, X.P.: Study on L1 over L2 minimization for nonnegative signal recovery. Journal of Scientific Computing **95**(3), 94 (2023)

[39] Tibshirani, R.: Regression shrinkage and selection via the lasso. Journal of the Royal Statistical Society: Series B (Methodological) **58**(1), 267–288 (1996)

[40] Wainwright, M.J.: High-Dimensional Statistics: A Non-Asymptotic Viewpoint. Cambridge University Press (2019)

[41] Xu, F., Ma, J., Lu, H.: Group sparse enhanced indexation model with adaptive beta value. Quantitative Finance **22**(10), 1905–1926 (2022)

[42] Xu, Z., Chang, X., Xu, F., Zhang, H.: $l_{1/2}$ regularization: A thresholding representation theory and a fast solver. IEEE Transactions on Neural Networks and Learning Systems **23**(7), 1013–1027 (2012)

[43] Yuan, M., Lin, Y.: Model selection and estimation in regression with grouped variables. Journal of the Royal Statistical Society: Series B (Statistical Methodology) **68**(1), 49–67 (2006)

[44] Zhang, T.: Adaptive forward-backward greedy algorithm for learning sparse representations. IEEE Transactions on Information Theory **57**(7), 4689–4708 (2011)

[45] Zhang, T.: Sparse recovery with orthogonal matching pursuit under RIP. IEEE Transactions on Information Theory **57**(9), 6215–6221 (2011)

[46] Zhang, X., Zhang, X.: A new proximal iterative hard thresholding method with extrapolation for ℓ_0 minimization. Journal of Scientific Computing **79**(2), 809–826 (2019)

[47] Zhao, Z., Xu, F., Wang, M., Zhang, C.: A sparse enhanced indexation model with $\ell_{1/2}$ norm and its alternating quadratic penalty method. Journal of the Operational Research Society **70**(3), 433–445 (2019)